Taconic Metamorphism Preserved in the Baie Verte Peninsula, Newfoundland Appalachians: Geochronological Evidence for Ophiolite Obduction and Subduction and Exhumation of the Leading Edge of the Laurentian (Humber) Margin During Closure of the Taconic Seaw

Sébastien Castonguay, Cees R. van Staal, Nancy Joyce, Thomas Skulski and James P. Hibbard

See table of contents

Explore this journal

Cite this article

Castonguay, S., van Staal, C., Joyce, N., Skulski, T. & Hibbard, J. (2014). Taconic Metamorphism Preserved in the Baie Verte Peninsula, Newfoundland Appalachians: Geochronological Evidence for Ophiolite Obduction and Subduction and Exhumation of the Leading Edge of the Laurentian (Humber) Margin During Closure of the Taconic Seaw. *Geoscience Canada*, *41*(4), 459–482. https://doi.org/10.12789/geocanj.2014.41.055

Article abstract

The Baie Verte Peninsula, western Newfoundland Appalachians, preserves evidence for Early to Mid Ordovician closure of the Taconic seaway, which led to obduction of the Baie Verte oceanic tract (BVOT) ophiolites onto the Laurentian (Humber) margin and Taconic orogenesis. The scarcity of Taconic radiometric ages (and predominance of Silurian (Salinic) data) from the Humber margin rocks (down-going plate) has been problematic, calling into question the intensity and existence of Taconic collisional orogenesis. 40Ar/39Ar and in situ U–Pb geochronology was undertaken on metamorphosed units from the Laurentian basement (Mesoproterozoic East Pond Metamorphic Suite), from the ca. 560 Ma Birchy Complex forming the leading edge of the Humber margin, and from the ca. 490 Ma ophiolitic rocks of the BVOT (Advocate Complex) in order to address this question. Our results confirm evidence of Taconic metamorphism along the Humber margin and at the base of the ophiolites. Ages obtained from the structural base of the Advocate Complex (481–465 Ma) are interpreted to reflect the timing of accretion and internal thickening of the ophiolite, whereas data from the underlying Birchy Complex (467–461 Ma) record the underthrusting and exhumation of the leading edge of the Humber margin along a subduction channel, penecontemporaneously with final obduction of the BVOT. A concordant ca. 465 Ma zircon age and REE data obtained from retrogressed eclogite of the East Pond Metamorphic Suite suggest that the parautochthonous Humber margin was locally subducted to eclogite-facies conditions during the Taconic collision and partly exhumed to amphibolite-facies conditions prior to a strong Silurian (Salinic) tectonometamorphic overprint.

HAROLD WILLIAMS SERIES
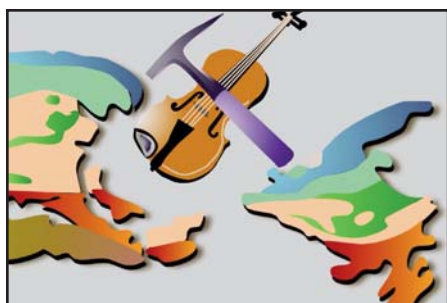
Taconic Metamorphism Preserved in the Baie Verte Peninsula, Newfoundland Appalachians: Geochronological Evidence for Ophiolite Obduction and Subduction and Exhumation of the Leading Edge of the Laurentian (Humber) Margin During Closure of the Taconic Seaway

Sébastien Castonguay[1], Cees R. van Staal[2], Nancy Joyce[3], Thomas Skulski[3], and James P. Hibbard[4]

[1]*Geological Survey of Canada*
Natural Resources Canada
Québec, Québec, G1K 9A9, Canada
E-mail: sebastien.castonguay@nrcan-rncan.gc.ca

[2]*Geological Survey of Canada*
Natural Resources Canada, Vancouver
British Columbia, V6B 5J3, Canada

[3]*Geological Survey of Canada*
Natural Resources Canada
Ottawa, Ontario, K1A 0E8, Canada

[4]*Department of Marine, Earth and Atmospheric Sciences*
North Carolina State University
Raleigh, North Carolina, 27695-8208, USA

SUMMARY

The Baie Verte Peninsula, western Newfoundland Appalachians, preserves evidence for Early to Mid Ordovician closure of the Taconic seaway, which led to obduction of the Baie Verte oceanic tract (BVOT) ophiolites onto the Laurentian (Humber) margin and Taconic orogenesis. The scarcity of Taconic radiometric ages (and predominance of Silurian (Salinic) data) from the Humber margin rocks (down-going plate) has been problematic, calling into question the intensity and existence of Taconic collisional orogenesis. $^{40}Ar/^{39}Ar$ and *in situ* U–Pb geochronology was undertaken on metamorphosed units from the Laurentian basement (Mesoproterozoic East Pond Metamorphic Suite), from the ca. 560 Ma Birchy Complex forming the leading edge of the Humber margin, and from the ca. 490 Ma ophiolitic rocks of the BVOT (Advocate Complex) in order to address this question. Our results confirm evidence of Taconic metamorphism along the Humber margin and at the base of the ophiolites. Ages obtained from the structural base of the Advocate Complex (481–465 Ma) are interpreted to reflect the timing of accretion and internal thickening of the ophiolite, whereas data from the underlying Birchy Complex (467–461 Ma) record the underthrusting and exhumation of the leading edge of the Humber margin along a subduction channel, penecontemporaneously with final obduction of the BVOT. A concordant ca. 465 Ma zircon age and REE data obtained from retrogressed eclogite of the East Pond Metamorphic Suite suggest that the parautochthonous Humber margin was locally subducted to eclogite-facies conditions during the Taconic collision and partly exhumed to amphibolite-facies conditions prior to a strong Silurian (Salinic) tectonometamorphic overprint.

SOMMAIRE

La péninsule de Baie Verte dans les Appalaches de l'ouest de Terre-Neuve a conservé des indices de la fermeture du bras de mer taconique, qui a mené à l'obduction des ophiolites de la bande océanique de Baie Verte (BOBV) sur la marge laurentienne (Humber) et à l'orogénèse taconique. La rareté des âges radiométriques taconiques (et la prédominance des données siluriennes (saliniques)) provenant des roches de la marge de Humber (i.e. la plaque subductée) a été problématique, mettant en question l'intensité et l'existence de la collision orogénique taconique. De la géochronologie $^{40}Ar/^{39}Ar$ et U–Pb *in situ* a été réalisée sur des unités métamorphisés provenant du socle laurentien (la Suite Métamorphique d'East Pond d'âge Mésoprotérozoïque), du Complexe de Birchy daté à ca. 560 Ma formant la partie frontale de la marge de Humber, et des roches ophiolitiques de la BOBV (Complexe d'Advocate) datée à ca. 490 Ma afin de

confronter ce questionnement. Nos résultats confirment les indices de métamorphisme taconique le long de la marge de Humber et à la base des ophiolites. Les âges obtenus à la base structurale du Complexe d'Advocate (481–465 Ma) sont interprétés comme reflétant la période d'accrétion et d'épaississement interne de l'ophiolite, tandis que les données du Complexe de Birchy sous-jacent (467–461 Ma) enregistrent le sous-charriage et l'exhumation de la partie frontale de la marge de Humber au sein d'un chenal de subduction, de façon pénécontemporaine à l'obduction finale de la BOBV. Un âge concordant de ca. 465 Ma d'un zircon et les données de terres rares provenant d'une éclogite rétromorphosée de la suite métamorphique d'East Pond suggèrent que la marge de Humber parautochtone a été localement subductée à des conditions du faciès éclogitique durant la collision taconique et partiellement exhumée à des conditions du faciès des amphibolites précédant la forte surimposition tectonométamorphique silurienne (salinique).

INTRODUCTION

Williams (1977) recognized that the Baie Verte Peninsula, specifically the Birchy Complex, was a key area to understand the geological processes involved in the Taconic arc–continent collision between the Laurentian margin and the outboard Notre Dame arc. He also realized that constraining the age of deformation and metamorphism associated with Taconic orogenesis was one of the major issues of Appalachian geology. Since then, radiometric age dating of metamorphic tectonites occurring in the structural wedge developed on the Laurentian margin in Newfoundland have predominantly yielded Silurian Salinic (Cawood et al. 1994; Lin et al. 2013) and younger ages, which challenge the strong structural, petrological and sedimentological evidence that these rocks were subjected to Ordovician tectonism at an earlier stage (e.g. Dallmeyer 1977; Cawood and Suhr 1992; van Staal et al. 2007). This has called into question the intensity and nature of Taconic orogenesis (Cawood et al. 1994) and suggested that Taconic suturing may have been incomplete and convergence continued due to sub-

duction driven by trapped oceanic lithosphere along strike.

Radiometric dating of metamorphic minerals formed during the early phases of tectonic burial associated with terrane accretion and collision in poly-deformed orogenic belts is notoriously difficult and challenging. This is due to common complete overprinting of the initial paragenesis and resetting of isotopic systems during subsequent metamorphism that is associated with thermal relaxation, exhumation and/or resulting from younger unrelated tectonometamorphic events (e.g. Villa 2004). Evidence of the nature and timing of the early tectonometamorphic processes is locally preserved in tectonic settings where partially subducted crust was exhumed relatively early during convergence and/or, collision, translating the metamorphic rocks to higher levels in the crust above the closure temperatures of isotopic geochronometers. Exhumation may have involved processes such as tectonic extrusion, eduction, extension, syntectonic erosion or combinations thereof, all of which could be driven by forces related to changing plate dynamics such as slab retreat, channel flow or slab breakoff (see Hacker and Gerya 2013 or Jamieson and Beaumont 2013 for reviews).

To better understand the tectonic cause of the lack of evidence for Ordovician metamorphism, we investigated the timing of tectonometamorphism along the Taconic paleo-suture on the Baie Verte Peninsula. This area preserves parts of the hyperextended Laurentian continental margin (e.g. Birchy Complex, van Staal et al. 2013), East Pond Metamorphic Suite, (Hibbard 1983; de Wit and Armstrong 2014) and fragments of obducted Baie Verte oceanic tract (BVOT) ophiolite (e.g. Advocate ophiolite complex). The exceptional preservation of the early D_1 structures suggested that this area may have escaped the intense overprinting by Salinic orogenesis, similar to parts of southern Quebec and northern Vermont Appalachians (Castonguay et al. 2001, 2012). In this contribution we present new $^{40}Ar/^{39}Ar$ and *in situ* U–Pb zircon ages from polymetamorphic units of the Baie Verte Peninsula. These ages confirm that significant burial and tectonometamor-

phism of the Laurentian margin took place during the Ordovician Taconic orogeny and that these units were rapidly exhumed above isotopic closure temperatures prior to Salinic tectonometamorphic overprint.

TECTONOSTRATIGRAPHIC SETTING

The Baie Verte Peninsula (Fig. 1) straddles the boundary between the Humber Zone, the remnant of the ancient continental margin of Laurentia (referred to as Humber margin from here on), and the diverse ophiolitic complexes and cover rocks of the BVOT of the Notre Dame Subzone (western Dunnage Zone; Williams et al. 1988), which mainly represent peri-Laurentian arc systems and related environments. The BVOT is interpreted to represent the vestiges of a relatively narrow seaway (Taconic seaway of Hibbard et al. 2007) that developed between Laurentia proper and isolated ribbon-like zones of continental crust of Laurentian affinity, collectively forming the Dashwoods microcontinent (Waldron and van Staal 2001; van Staal et al. 2013). This rifted ribbon of continental crust eventually formed the substrate for younger magmatic arc sequences (e.g. Notre Dame arc; van Staal et al. 2007). The tectonic boundary between the Humber Zone and Notre Dame Subzone is marked by the Baie Verte Line (northern extension of the Baie Verte–Brompton Line of Williams and St. Julien 1982), a complex, poly-phase, brittle–ductile shear zone that now separates obducted ophiolitic crust and mantle from the Laurentian continental margin.

West of the Baie Verte Line, the Humber Zone comprises the East Pond Metamorphic Suite (de Wit 1980; Hibbard 1983), consisting of migmatite, ortho- and paragneiss and Middle Arm metaconglomerate, respectively shown to represent ca. 1490 Ma Pinwarian basement that was overprinted by Grenvillian metamorphism (de Wit and Armstrong 2014) and an unconformably overlying unit, which forms the base of the Fleur de Lys Supergroup (Fig. 1). The Fleur de Lys Supergroup consists of psammite, pelite, marble and mafic schist, deposited on or near the continental margin (Bursnall and de Wit 1975; Hibbard 1983; Hibbard et al. 1995).
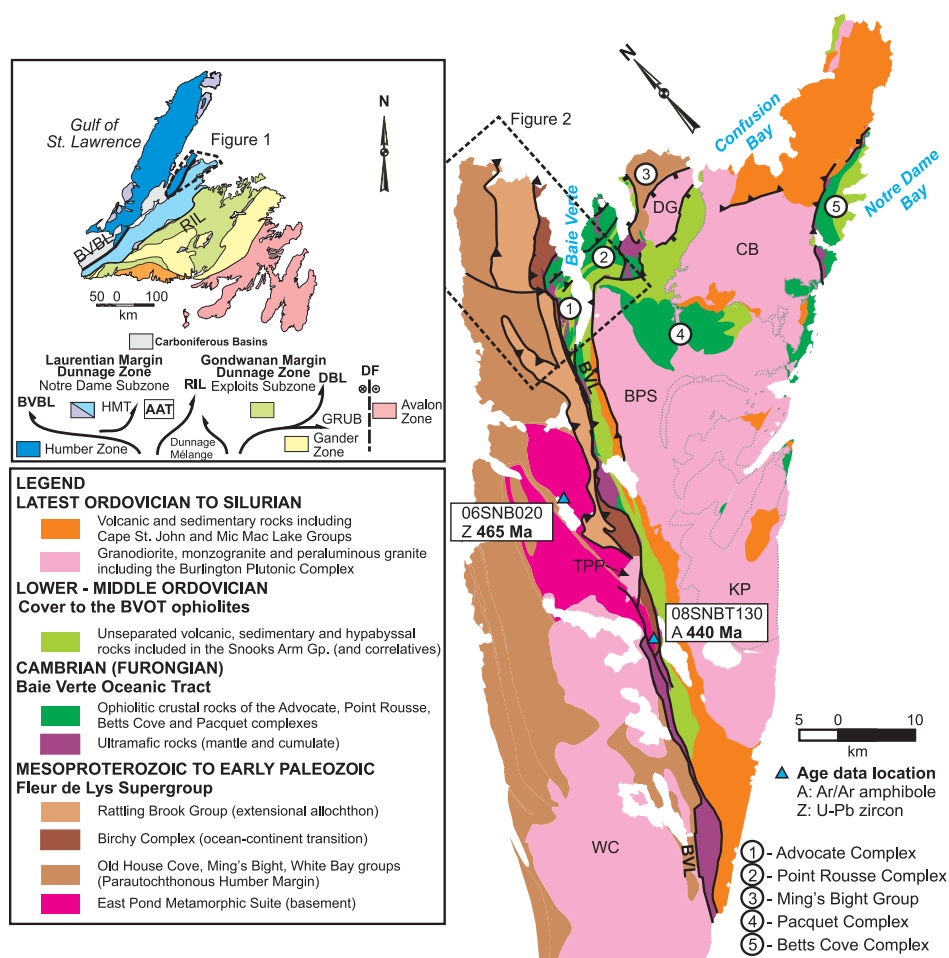
Figure 1. Simplified geology of the Baie Verte Peninsula, northwestern Newfoundland (modified from Hibbard 1983; Skulski et al. 2010; van Staal et al. 2013) with age data locations. AAT: Annieopsquotch accretionary tract; BPS: Burlington plutonic suite; BVBL: Baie Verte–Brompton Line; BVL: Baie Verte Line and Baie Verte Road fault; CB: Cape Brule Porphyry; DBL: Dog Bay Line; DF: Dover Fault; DG: Dunamagon Granite; GRUB: Gander River Ultramafic Belt; HMT: Hungry Mountain Thrust; KP: King's Point Complex; RIL: Red Indian Line; TPP: Trap Pond pluton; WC: Wild Cove Pond Igneous Suite.

From west to east, the supergroup includes the White Bay, Old House Cove, Rattling Brook groups and the Birchy Complex (Figs. 1 and 2). The latter three include relatively small serpentinized ultramafic slivers and are considered to represent the remnants of the leading edge of the hyperextended Humber margin (Hibbard 1983; van Staal et al. 2013). Correlatives of the Fleur de Lys Supergroup are exposed to the east of the Baie Verte Line where they have been included in the Ming's Bight Group (Fig. 1). The Ming's Bight Group comprises metapelite, psammite, amphibolite and rare ultramafic fuchsite–actinolite schist that are exposed in the core of a tectonic window (Anderson et al. 2001).

Several ophiolite sequences of the BVOT are exposed to the east of the Baie Verte Line. These include the relatively intact ca. 489–487 Ma (Dunning and Krogh 1985; Skulski et al. 2010) Betts Cove Complex (Bédard et al. 2000), and dismembered correlative units including the 487 Ma Pacquet Complex, the 489 Ma Point Rousse Complex, and the Advocate Complex (Fig. 1; Hibbard 1983; Skulski et al. 2010, 2012a). The BVOT ophiolites are disconformably overlain by Floian to Dapingian (ca. 476–467 Ma.; Skulski et al. 2010, 2012a) volcano-sedimentary cover sequences comprising the

Snooks Arm Group that include the former upper Pacquet Harbour Group, the Point Rousse cover sequence, the Flat Water Pond and Shark Point groups, and the Snooks Arm Group as originally defined (cover units to the Betts Cove Complex; Bursnall 1975, Hibbard 1983; Bédard et al. 2000; Skulski et al. 2010, 2012a). The youngest marine volcano-sedimentary sequence includes the Black Brook formation dated at ≤457 Ma (Skulski et al. 2012b).

The Baie Verte oceanic tract and Humber Zone are intruded by Late Ordovician to Early Silurian (Llandovery) granitoid plutons including the ca. 445–433 Ma Burlington plutonic suite, ca. 429 Ma Cape Brulé porphyry, ca. 427 Ma Dunamagon Granite, ca. 428 Ma Wild Cove Pond Igneous Suite and ca. 423 Ma Trap Pond pluton (Fig. 1; Cawood and Dunning 1993, Skulski et al. 2012b). These plutons are in part consanguineous with the Late Ordovician to Early Silurian, continental volcanic and sedimentary cover sequences that unconformably overlie previously deformed Ordovician and Silurian units on the peninsula. For example, the Burlington plutonic suite is locally unconformably overlain by sedimentary and volcanic rocks of the Micmac Lake Group (ca. 442 to >430 Ma: Kidd 1974, Skulski et al. 2012b). The Cape St. John Group lies unconformably on the Snooks Arm Group further to the east (e.g. Neale et al. 1975) and comprises continentally derived sedimentary rocks and bimodal volcanic rocks including ca. 428–426 Ma felsic volcanic rocks (Fig. 1; Skulski et al. 2010, 2012b).

The Birchy Complex
The Birchy Complex (Bursnall 1975; Williams 1977; Hibbard 1983; Winchester et al. 1992) consists of a ca. 1 to 2.5 km wide belt of polymetamorphosed (greenschist to locally amphibolite facies) and polydeformed mafic schist and gabbro, interlayered psammite, graphitic pelite and ultramafic rocks (serpentinized peridotite, altered pyroxenite and tremolite-fuchsite schist), which are structurally sandwiched between overlying ophiolite massifs of the BVOT (along the Baie Verte Line) and structurally underlying younger metasedimentary rocks of the

Rattling Brook Group (Fleur de Lys Supergroup; Figs. 1 and 2). A gabbro of the Birchy Complex yielded a Late Ediacaran U–Pb zircon ID–TIMS age of 558.3 ± 0.7 Ma, whereas LA–ICP–MS concordia zircon ages of a gabbro and intermediate tuffaceous schist gave ages of 564 ± 7.5 Ma and 556 ± 4 Ma, respectively (van Staal et al. 2013). Gabbro intruded the ultramafic rocks, indicating a genetic rather than a structural relationship. Clastic rocks that are interleaved with the Birchy Complex schist contain chromite detritus indicating that the ultramafic rocks were exhumed, eroded and deposited onto the seafloor during Birchy Complex magmatism and sedimentation.

The preservation of ophiolitic affinity rock types, close association with clastic units typical of the Fleur de Lys Supergroup, and dismembered tectonic character, led to interpretation of the Birchy Complex as a zone of tectonic mélange (Bursnall 1975; Hibbard et al. 1995) or ophiolitic depositional mélange (Williams 1977) that accommodated the initial stages of ophiolite obduction onto the Humber margin (Bursnall 1975; Williams 1977; Hibbard et al. 1995). Recently, van Staal et al. (2013) have advocated that the Birchy Complex represents the remnants of an ocean–continent transition zone formed by hyperextension of the Humber margin during the opening of the Taconic seaway, which was subsequently complexly deformed during its Taconic closure.

Advocate Complex

The Advocate Complex is the westernmost, and most structurally disrupted and deformed part of the BVOT on the Baie Verte Peninsula (Figs. 1 and 2; Hibbard 1983; Skulski et al. 2010). It consists of several fault-bounded megaslivers that demarcate the Baie Verte Line and comprise serpentinized mantle harzburgite with discordant dunite pods and dykes, mostly in tectonic contact with boninitic, serpentinized ultramafic cumulate rocks, layered gabbro, boninitic anorthositic gabbro (in part transformed into clinozoisite-quartz rock), gabbro, sheeted dykes and rare, tectonic slices of mafic volcanic rocks (Skulski et al. 2010). Most of the pillowed volcanic section of the ophiolite is not preserved either
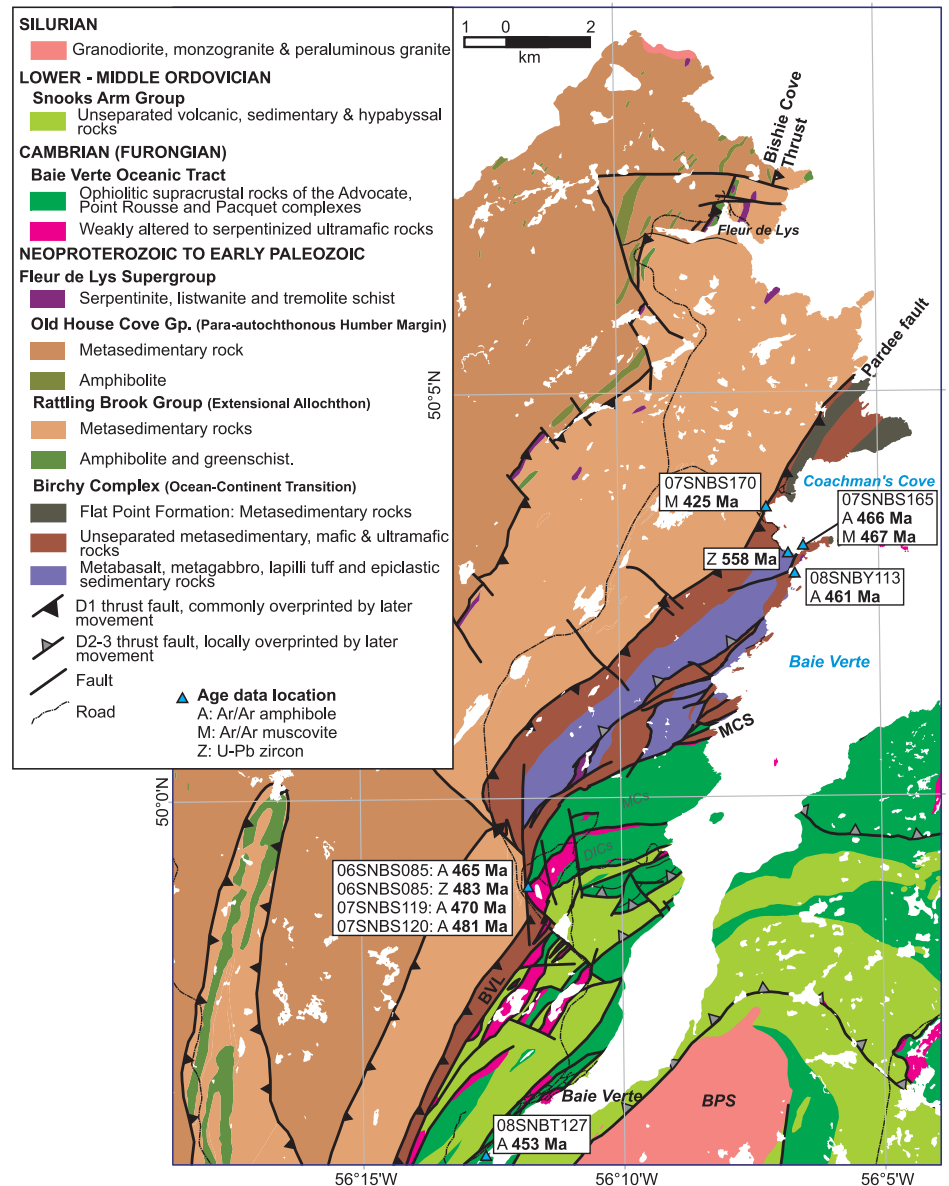

Figure 2. Simplified geology of the northwestern part of the Baie Verte Peninsula (modified from Hibbard 1983, Skulski et al. 2010; van Staal et al. 2013) with age data locations in the Birchy and Advocate complexes. BPS: Burlington plutonic suite; BVL: Baie Verte Line and Baie Verte Road fault; DICs: Duck Island Cove sequence; MCS: Marble Cove Slice; MCs: Marble Cove sequence.

due to faulting and/or erosion. The base of the adjacent Snooks Arm Group comprises a clastic detrital wedge in part derived from the ophiolite (Kidd 1974; Skulski et al. 2010; 2012a).

Eclogite and Amphibolite of the Humber Zone

The East Pond Metamorphic Suite and Fleur de Lys Supergroup commonly contain centimetre- to decametre-scale amphibolite and eclogite layers, pods and lenses or boudins (Hibbard 1983).

Cross-cutting relationships with metasedimentary rocks attest that most amphibolite originated as mafic dykes or sills, although locally gradational contacts with host metasedimentary rocks suggest that some may be mafic flows or volcaniclastic layers (de Wit and Strong 1975; Hibbard 1983). Partly amphibolitized, boudinaged bodies of eclogite occur in the East Pond Metamorphic Suite (Neale and Kennedy 1967; de Wit and Strong 1975) and within the overlying Middle Arm Metaconglomerate (i.e. base of the Fleur de

Lys Supergroup; Neale and Kennedy 1967; Church 1969; Hibbard 1983). The cores of these bodies locally preserve eclogitic mineral assemblages including garnet, omphacite, quartz, rutile, hornblende, phengite and zoisite. The eclogitic metamorphic assemblage is interpreted to have developed at 450–500ºC and at least 10–12 kbar, and later re-equilibrated at 700–750ºC and 7–9 kbar (Jamieson 1990).

TECTONOMETAMORPHIC EVOLUTION

Notwithstanding basement tectonometamorphism (pre-Fleur de Lys Supergroup) of the East Pond Metamorphic Suite that produced migmatite and gneiss (de Wit 1980; Jamieson 1990), the complex and episodic tectonometamorphic evolution of the Fleur de Lys Supergroup (Jamieson and Vernon 1987; Stallard 1998) and Baie Verte oceanic tract can be grouped into four phases of regional deformation and three metamorphic pulses (Bursnall and de Wit 1975; Hibbard 1983; Jamieson 1990; Castonguay et al. 2010). Most deformation phases and metamorphic imprints are domainal and fabrics vary in orientation, style and in intensity. In addition, correlations across the Baie Verte Line are rendered difficult due to intense and long-lived deformation, which resulted in juxtaposition of rock units of different origins and tectonometamorphic levels.

      Structures related to D_1 (D_E of Hibbard 1983) have been strongly overprinted in the Fleur de Lys Supergroup, and are poorly developed in the BVOT. They consist of a transposed metamorphic differentiated or micaceous fabric, typically bedding-parallel, preserved as intrafolial folds or in fold interference patterns involving F_2 and F_3 (Kennedy 1971; Hibbard 1983). In spite of tight to isoclinal refolding by F_2, S_1 is commonly the dominant foliation in the Rattling Brook Group and especially so in the Birchy Complex where it is defined by a differentiated metamorphic layering (Fig. 3A; and figure 4D, F of van Staal et al. 2013). D_1 fabrics are associated with a series of early shear zones, termed 'slide zones' in the literature (Kennedy 1971; Kidd 1974; Bursnall 1975), which are often
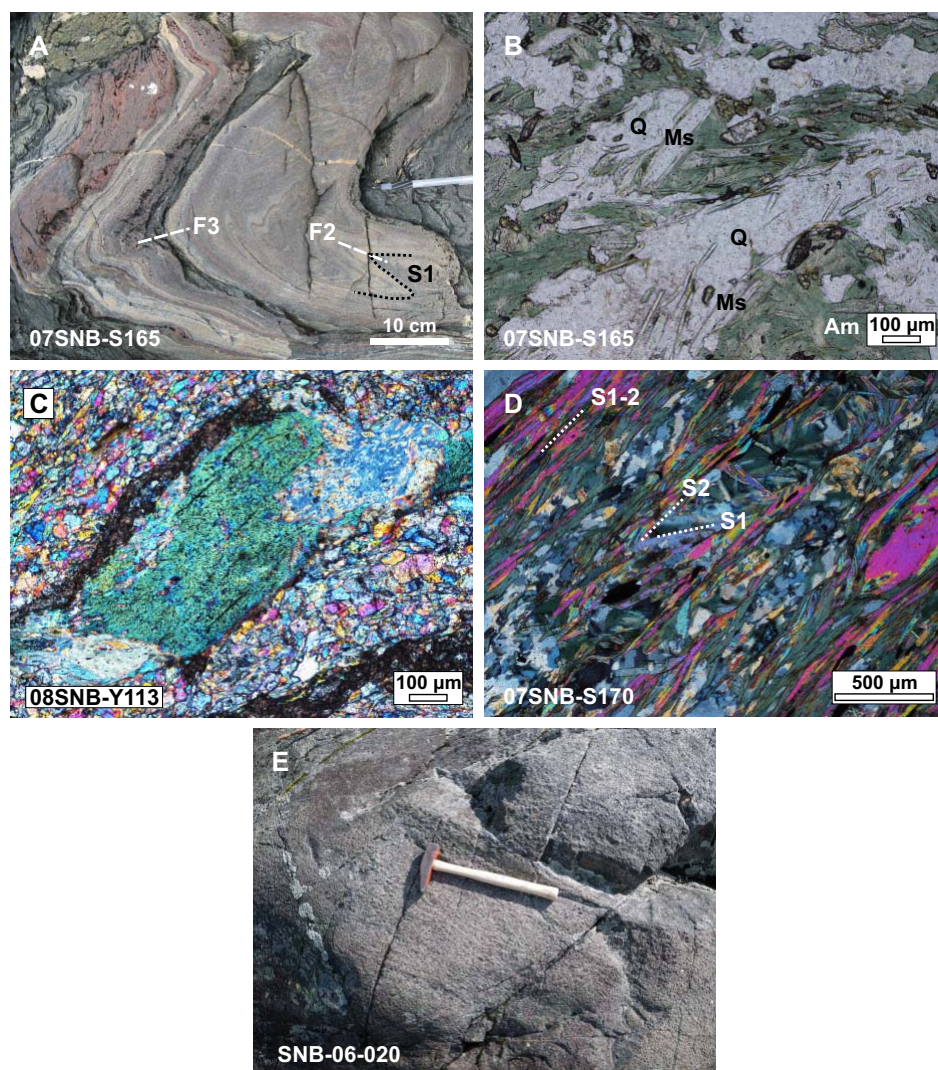

Figure 3. Representative photographs of dated Birchy Complex (A to D) and eclogite (E) localities and thin sections. A: Complexly folded (F_2 and F_3 of predominant S_1) mafic schist with lenses of jasper and epidosite (sample 07SNB-S165). B: Photomicrograph (plane-polarized light) of sample 07SNB-S165 showing epidote- and hornblende-bearing mafic schist, with possible quartz-muscovite veinlets. Am: Amphibole; Ms: Muscovite; Q: Quartz. C: Photomicrograph (crossed polars) of a typical amphibole porphyroblast of the gabbro sample 08SNB-Y113. D: Photomicrograph (crossed polars) showing the strongly developed S2 fabric overprinting S1, only locally differentiated, from the psammite sample of locality 07SNB-S170. E: Dated eclogite body along the north end of Gull Pond (Hibbard 1983). Retrogression of the weakly foliated eclogite to amphibolite is moderate, but becomes progressively more pronounced towards the contact with the strongly foliated enveloping gneiss and schist of the East Pond Metamorphic Suite. The amphibolitized eclogite is interpreted as a polymetamorphosed mafic dyke. See Figures 1 and 2 for sample locations.

marked by serpentinized ultramafic slivers derived from pre-orogenic, exhumed lithospheric mantle (Fig. 2; van Staal et al. 2013). White mica associated with S_1, part of a chloritoid-bearing assemblage, is consistently more phengitic (e.g. Si^{4+} 6.75–6.53 based on 22 oxygens; Jamieson 1990)

than the later generation of muscovite (e.g. Si^{4+} 6.53–6.27). D_1 was associated with greenschist-facies metamorphism, with local evidence for amphibolite-facies conditions (Hibbard 1983). Early metamorphism recorded in the eclogite of the East Pond Metamorphic Suite reached conditions of 10–12 kbar min-
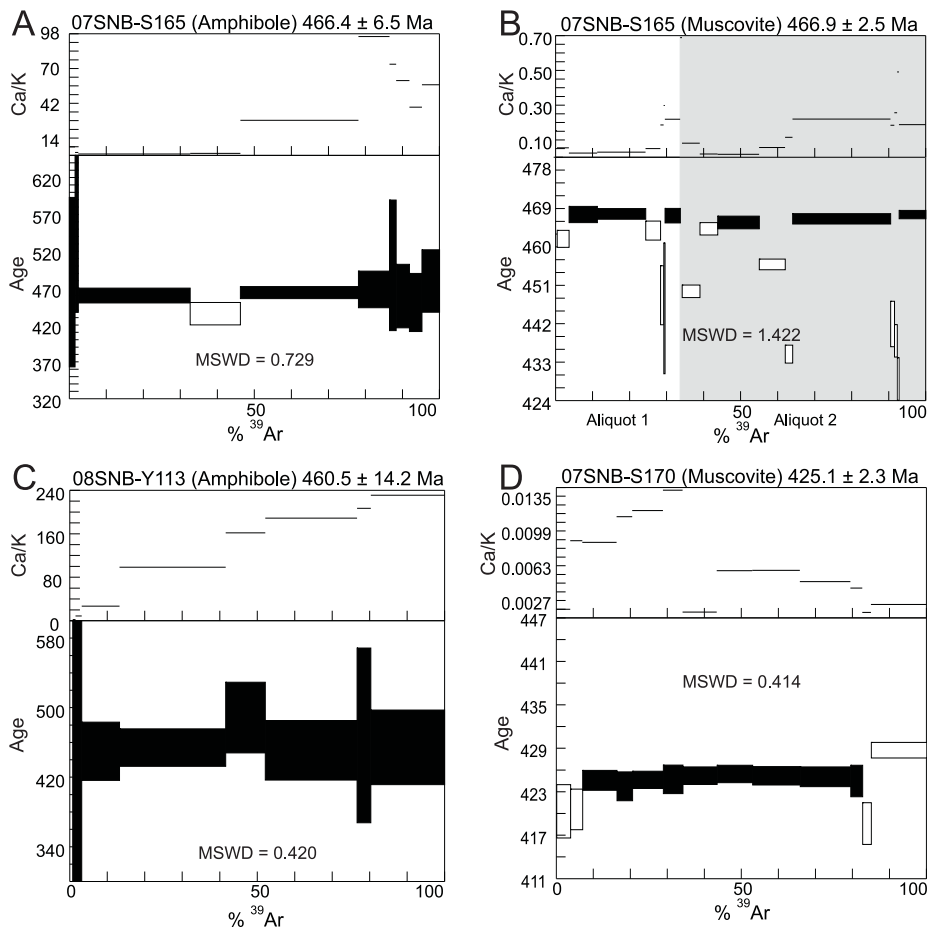
Figure 4. $^{40}Ar/^{39}Ar$ step-heating spectra (all steps are presented at 2σ relative uncertainties) and $^{37}Ar_{Ca}/^{39}Ar_K$ ratio diagrams of Birchy Complex samples. Plateau segments are shown in black. Plateau age uncertainties are 2σ and include both analytical and J-factor errors. A: Amphibole aliquot from sample 07SNB-S165. B: Combined muscovite aliquots from sample 07SNB-S165. C: Amphibole aliquot from sample 08SNB-Y113. D: muscovite aliquot from sample 07SNB-S170. See Figure 2 for sample locations. MSWD: mean square of weighted deviates.

imum and 450–500°C prior to an amphibolite-facies overprint at 700–750°C and 7–9 kbar, the latter considered contemporaneous with earliest prograde metamorphism in the overlying Fleur de Lys Supergroup (7–9 kbar and ca. 450–500°C; de Wit 1980; Jamieson 1990; Jamieson and O'Beirne-Ryan 1991). More recently, Willner et al. (2012) obtained much higher peak pressure values and estimated that the garnet-mica schist of the Fleur de Lys Supergroup and eclogite pods of the East Pond Metamorphic Suite have reached conditions of 18 and 20 kbar, respectively. D_1 is interpreted to relate to obduction of ophiolite complexes of the BVOT first over isolated, allochthonous slivers of the hyperextended Humber margin (e.g. Rattling Brook block), followed by

the attempted subduction of the autochthonous margin during the main phase of Taconic orogeny (Hibbard 1983; Waldron et al. 1998; van Staal et al. 2007, 2013).

The D_2 event (Dm of Bursnall and de Wit 1975 and Hibbard 1983) represents the main tectonometamorphic phase of most of the Baie Verte Peninsula, which imparted a penetrative, dominantly northeast-trending structural grain to Fleur de Lys Supergroup. It folded basement and cover into large amplitude upright structures, best outlined by basement-cored, shallowly north-plunging antiforms in the western part of the Baie Verte Peninsula (Fig. 2; Kennedy 1971; Bursnall and de Wit 1975; de Wit 1980; Hibbard 1983; de Wit and Armstrong 2014). In the East Pond Metamorphic

Suite, S_2 is generally a steeply dipping penetrative fabric and it is intensely developed at contacts with the Fleur de Lys Supergroup. In the latter, the D_2 fabrics are represented by a moderately to steeply dipping schistosity, axial planar to tight to isoclinal NNE- to SSW-plunging folds, strongly transposing S_1. In parts of the Birchy Complex, S_2 is manifested as a widely spaced crenulation cleavage preserving S_1 in the micro-scale F_2 hinges, or as a foliation developed by the transposition of S_1 into parallelism with F_2 axial planes.

D_2 shear zones, some of which reused earlier D_1 faults, are locally associated with attenuated limbs of major F_2 folds. Kinematics of these shear zones are generally complex or obscured by superimposed strains, especially adjacent to long-lived faults associated with the Baie Verte Line (Hibbard 1983; Piasecki 1988; Goodwin and Williams 1996). Shear zones occurring at the mylonitic contacts between the East Pond Metamorphic Suite and the Fleur de Lys Supergroup (Piasecki 1988) were folded by F_2 folds, so that their kinematics and timing are uncertain. D_2 faults are ESE-directed along the contact between the BVOT and the Burlington plutonic suite (Kidd 1974), however, the vergence of D_2 structures in the northwest part of the Birchy Complex and adjacent Rattling Brook Group (where post-D_2 strain is generally weaker) suggest northwest-directed transport (Kidd 1974; Bursnall 1975; Hibbard 1983).

Peak regional metamorphism attained upper greenschist to lower amphibolite facies and is interpreted to have taken place syn- to late D_2. Regionally, rocks of the Fleur de Lys Supergroup are characterized by the growth of late M_2 albite and garnet (± biotite, chloritoid, kyanite, staurolite and pyroxene) porphyroblasts (Hibbard 1983; Jamieson and Vernon 1987; Jamieson and O'Beirne-Ryan 1991; Stallard 1998; Stallard and Hickey 2002). Porphyroblasts have been interpreted to have formed during a phase of decompression and heating at ca. 550°C and 6.5 kbar (Jamieson 1990).

The D_3 event (D_L of Hibbard 1983) produced ductile–brittle shear zones that are associated with domainal deformation zones occurring in the Birchy and Advocate complexes

where S_3 and F_3 are penetratively developed (Bursnall and de Wit 1975). D_3 shear zones locally accommodated southeast-directed thrusting, in part reactivating D_2 faults (Fig. 2; Bursnall 1975; Piasecki 1988). The subvertical S_3 foliation varies from a non-penetrative crenulation cleavage to a penetrative schistosity. Associated, open to tight F_3 folds are commonly chevron-style structures with angular hinges. D_3 fabrics are consistently oriented more clockwise (easterly) than those of D_2. Growth of metamorphic minerals is negligible or confined to rotated and/or recrystallized micas along S_3 (Kidd 1974), suggesting that D_3 is post-peak metamorphism in the Fleur de Lys Supergroup. The D_2 and D_3 structural phases are interpreted to form part of a progressive deformation associated with the Salinic orogeny (Skulski et al. 2010), which led to strain partitioning in an overall sinistral transpressional regime (Anderson 1998; Waldron et al. 1998). This complex progressive deformation contributed to the exhumation of the Fleur de Lys Supergroup (Jamieson 1990; Cawood et al. 1995). This deformation appears to be coeval with south-directed thrusting and thickening of BVOT ophiolitic and cover rocks east of the bay of Baie Verte (Point Rousse and Pacquet complexes; Waldron et al. 1998; Anderson 1998; Skulski et al. 2010).

The D_4 event (also part of D_L of Hibbard 1983) is manifested by late fabrics associated with the development and reactivation of steep NNE-trending fault zones marking the Baie Verte Line, termed the Baie Verte Road fault system (Hibbard 1983). The latter and its northeastern extension (the Marble Cove Slide of Bursnall 1975; Fig. 2), represent a long-lived complex fault zone that culminated with dextral kinematics (Goodwin and Williams 1996). East of the Baie Verte Line, D_4 structures are mainly recognized in the northern part of the peninsula as shallowly inclined to recumbent folds, cogenetic with northwest- and southeast-dipping ductile–brittle extensional shear zones (Fig. 1; D_2 of Anderson et al. 2001). D_4 is well developed along the contacts between the Ming's Bight Group and overlying BVOT units, where it is asso-

ciated with an amphibolite-facies metamorphic assemblage (Anderson 1998; Anderson et al. 2001). The D_4 regional deformation is associated with an overall dextral strike-slip (transpressional to transtensional) regime during the Acadian orogeny (Waldron et al. 1998; Anderson et al. 2001).

GEOCHRONOLOGY
Previous Data
Previous geochronological studies of the Fleur de Lys Supergroup and surrounding units did not obtain clear age constraints on the Taconic metamorphic imprint (Dallmeyer 1977; Mattinson 1977; Hibbard 1983; Dallmeyer and Hibbard 1984; Vance and O'Nions 1990, Cawood and Dunning 1993; Cawood et al. 1994; Anderson et al. 2001). $^{40}Ar/^{39}Ar$ analyses of the Fleur de Lys Supergroup rocks west of the Baie Verte Line indicate north-younging results of 428 ± 5 to 393 ± 5 Ma for hornblende, 424 ± 5 to 398 ± 5 Ma for muscovite, and 394 ± 5 to 374 ± 5 Ma for biotite (Dallmeyer 1977; recalculated using revised isotopic ratios, decay constants and standard ages in Dallmeyer and Hibbard 1984 and in this study). These are generally interpreted to record diachronous post-M_2 metamorphic cooling. More recent studies (Cawood and Dunning 1993; Cawood et al. 1994, 1995; recalculated in Skulski et al. 2012b) obtained U–Pb monazite ages of 428 ± 2 and 423 ± 2 Ma from a syn-tectonic (D_2) Wild Cove Pond Igneous Suite and late-kinematic Trap Pond pluton, respectively. Migmatite derived from the Fleur de Lys Supergroup yielded a 428 ± 2 U–Pb monazite age. These ages indicate that intrusion and peak metamorphism related to D_2 occurred during the Wenlock–Ludlow interval. These intrusions cut some of the structures associated with the basement-cored F_2 antiforms, but are locally also deformed by the same event (Kidd 1974; Hibbard 1983). East of the Baie Verte Line, $^{40}Ar/^{39}Ar$ and U–Pb dating of amphibolite schist, mafic dykes and pegmatite dykes in the Ming's Bight Group yielded ages ranging from 405 ± 8 to 355 ± 2 Ma (Anderson et al. 2001). Anderson et al. (2001) have interpreted these anomalously young ages to record tectonometamorphism and exhumation

localized in a transtensional setting associated with continuous dextral movements during D_4.

Experimental Procedure
$^{40}Ar/^{39}Ar$ Geochronology
Samples were processed for $^{40}Ar/^{39}Ar$ analysis using standard mineral separation techniques, including hand-picking of inclusion-free unaltered crystals in the 300–1000 μm size range. The grains were loaded into aluminum foil packets and arranged radially in an aluminum canister (40×19 mm) along with a several grains of Fish Canyon Tuff Sanidine (FCT–SAN) to act as flux monitor (apparent age = 28.201 ± 0.046 Ma (2σ); Kuiper et al. 2008). The samples were irradiated in two different batches for 40 MWh in position 5c at the research reactor of McMaster University (Hamilton, Ontario).

Laser $^{40}Ar/^{39}Ar$ step-heating and spot-dating analyses of the irradiated samples were carried out at the Geological Survey of Canada in Ottawa. For step heating, the samples were loaded into 1.5 mm diameter holes in a copper planchet and stepwise heated under vacuum using a Merchantek MIR10 10W CO_2 laser equipped with a 2 x 2 mm flat-field lens. The released Ar gas was cleaned over getters for ten minutes before isotope analysis using the secondary electron multiplier system of a VG3600 gas source mass spectrometer; details of data collection protocols can be found in Villeneuve and MacIntyre (1997) and Villeneuve et al. (2000). Error calculation on individual steps follows numerical error analysis routines outlined in Scaillet (2000), whereas error analysis on grouped data follows algebraic methods of Roddick (1988). Neutron flux gradients were evaluated by analyzing the FCT–SAN flux monitors for each tube, and by interpolating a linear fit against calculated J-factor and sample position. The error on the J-factor value reported in Table 1 is conservatively estimated at $\pm 0.6\%$ (2σ). Because this error is systematic and not related to individual analyses, correction for this uncertainty is not applied until calculation of dates from isotopic correlation diagrams (Roddick 1988). No evidence for excess ^{40}Ar was observed in any of the samples and, therefore, all regressions

Table 1. Laser step-heating ^{40}Ar/^{39}Ar data

Power[a]	Vol. ^{39}Ar x10^{-11} cc	^{36}Ar/^{39}Ar	±	^{37}Ar/^{39}Ar	±	^{38}Ar/^{39}Ar	±	^{40}Ar/^{39}Ar	±	%^{40}Ar ATM	*^{40}Ar/^{39}Ar	±	f$_{39}$[b] (%)	Apparent Age (Ma[c])	±
06SNB-S085A-02 Amphibole; J=.00476490[d] Advocate Complex (Z9291; 49.981778°N 56.196861°E)															
Aliquot: 1															
3.0	0.0136	2.5653	0.3456	7.705	1.700	0.636	0.115	1003.294	124.671	75.6	245.251	51.863	0.4	1408.6	205.8
4.0*	0.0536	0.2668	0.0297	33.492	1.167	0.066	0.022	138.751	5.124	56.8	59.899	9.096	1.7	456.2	60.8
5.0*	0.2712	0.0825	0.0059	12.078	0.293	0.037	0.013	85.028	1.666	28.7	60.651	2.107	8.5	461.2	14.1
5.5*	0.3944	0.0111	0.0040	8.468	0.185	0.046	0.012	63.925	0.714	5.1	60.641	1.377	12.4	461.2	9.2
6.0*	0.8115	0.0041	0.0023	9.045	0.144	0.054	0.011	62.712	0.704	1.9	61.509	0.969	25.5	467.0	6.5
6.5*	0.2482	0.0054	0.0073	9.632	0.181	0.050	0.013	62.746	0.966	2.5	61.149	2.365	7.8	464.5	15.7
7.5*	1.1221	0.0036	0.0024	10.889	0.134	0.049	0.011	62.647	0.476	1.7	61.589	0.851	35.3	467.5	5.7
15.0*	0.2637	0.0035	0.0056	14.135	0.289	0.048	0.012	60.846	1.122	1.7	59.820	2.000	8.3	455.6	13.4
07SNB-S119A-01 Amphibole; J=.00493380[d] (Z9605; 49.981833°N 56.196944°E)															
Aliquot: 1															
3.0	0.0775	0.1838	0.0144	2.263	1.741	0.181	0.018	146.940	3.644	37.0	92.635	4.806	1.7	684.1	29.4
3.5	0.1261	0.0349	0.0094	1.514	1.293	0.040	0.016	68.680	1.357	15.0	58.359	3.035	2.7	459.7	21.0
3.9	0.2055	0.0090	0.0049	1.616	0.666	0.013	0.011	61.082	1.233	4.3	58.432	1.881	4.4	460.2	13.0
4.6	0.5423	0.0015	0.0021	1.729	0.284	0.012	0.011	58.393	0.497	0.8	57.937	0.803	11.7	456.8	5.6
5.0*	1.7212	0.0036	0.0014	7.574	0.227	0.047	0.011	61.188	0.340	1.7	60.125	0.531	37.2	472.0	3.7
5.5*	0.8823	0.0027	0.0018	8.374	0.345	0.047	0.011	60.540	0.496	1.3	59.731	0.713	19.1	469.2	4.9
6.0*	0.4773	0.0032	0.0027	8.852	0.543	0.049	0.012	60.581	0.594	1.6	59.641	0.985	10.3	468.6	6.8
7.0*	0.1512	0.0002	0.0101	9.150	0.966	0.022	0.012	58.549	2.082	0.1	58.491	3.633	3.3	460.6	25.1
15.0*	0.4411	0.0014	0.0029	11.621	0.520	0.046	0.011	59.954	0.665	0.7	59.528	1.071	9.5	467.8	7.4
07SNB-S120A-01 Amphibole; J=.00493290[d] (Z9606; 49.983778°N 56.193806°E)															
Aliquot: 1															
3.0	0.0910	0.1555	0.0118	3.979	1.566	0.075	0.014	113.304	2.614	40.6	67.351	3.831	3.0	521.2	25.6
3.9	0.1453	0.1001	0.0107	6.794	1.327	0.067	0.016	91.184	2.034	32.4	61.617	3.441	4.9	482.2	23.5
4.6	0.3092	0.0045	0.0037	10.491	0.616	0.021	0.012	56.936	0.691	2.3	55.616	1.300	10.3	440.4	9.1
5.0	0.3712	0.0089	0.0061	32.326	1.016	0.056	0.011	74.375	0.840	3.6	71.734	1.978	12.4	550.5	13.0
5.5	0.0757	-0.0030	-0.0135	24.740	2.493	0.020	0.013	57.887	2.048	-1.5	58.760	4.496	2.5	462.4	31.0
6.5*	0.1013	-0.0059	-0.0151	46.958	2.347	0.038	0.013	74.946	2.020	-2.3	76.700	4.903	3.4	583.1	31.7
7.5*	0.0688	0.0007	0.0167	39.190	3.027	0.048	0.021	59.449	2.158	0.4	59.239	5.403	2.3	465.7	37.2
15.0*	0.1872	0.0121	0.0100	44.395	1.930	0.047	0.013	66.288	1.250	5.4	62.726	3.189	6.2	489.8	21.7
Aliquot: 2															
3.0*	0.0920	0.0391	0.0091	4.075	1.649	0.051	0.018	72.734	2.545	15.9	61.194	3.461	3.1	479.3	23.7
3.9*	0.1579	0.0214	0.0050	5.228	1.211	0.018	0.011	67.276	1.262	9.4	60.945	1.889	5.3	477.6	12.9
4.6*	0.4673	0.0067	0.0033	16.884	0.661	0.028	0.011	63.911	0.858	3.1	61.945	1.287	15.6	484.4	8.8
5.0*	0.1515	0.0070	0.0066	24.574	1.775	0.024	0.012	63.872	1.520	3.2	61.812	2.462	5.1	483.5	16.8
5.5	0.1116	-0.0017	-0.0082	13.941	1.273	0.027	0.013	55.171	1.658	-0.9	55.672	2.939	3.7	440.8	20.5
6.5	0.1097	-0.0032	-0.0054	18.561	1.484	0.010	0.015	52.925	1.448	-1.8	53.881	2.177	3.7	428.2	15.3
15.0*	0.5582	-0.0025	-0.0065	36.407	1.056	0.041	0.011	59.848	0.525	-1.2	60.584	1.994	18.6	475.1	13.7
07SNB-S165A-02 Muscovite; J=.00493160[d] (Z9607; 50.051611°N 56.107472°E)															
Aliquot: 1															
2.6	0.3449	0.0113	0.0041	0.080	0.014	0.014	0.011	54.849	0.656	6.1	51.521	1.368	0.4	411.3	9.7
3.0	2.8342	0.0007	0.0007	0.028	0.003	0.003	0.011	58.866	0.208	0.3	58.667	0.284	3.2	461.7	2.0
3.5*	6.7671	0.0006	0.0003	0.013	0.001	0.002	0.011	59.671	0.251	0.3	59.481	0.269	7.6	467.3	1.9
3.9*	11.5614	0.0002	0.0002	0.016	0.001	0.002	0.011	59.557	0.169	0.1	59.502	0.177	13.1	467.5	1.2
4.2	3.5659	0.0002	0.0006	0.026	0.002	0.000	0.011	59.013	0.270	0.1	58.942	0.317	4.0	463.6	2.2
4.6	0.7856	0.0016	0.0030	0.097	0.012	0.005	0.011	57.281	0.433	0.8	56.794	0.979	0.9	448.6	6.8
5.0	0.2953	0.0012	0.0066	0.155	0.029	0.001	0.011	56.699	0.937	0.6	56.359	2.163	0.3	445.5	15.1
15.0*	3.6564	0.0004	0.0006	0.114	0.003	0.001	0.011	59.548	0.180	0.2	59.444	0.244	4.1	467.1	1.7
Aliquot: 2															
2.6	0.4387	0.0071	0.0024	0.358	0.230	0.007	0.011	50.980	0.594	4.1	48.885	0.915	0.5	392.3	6.6
3.0	4.2454	0.0007	0.0002	0.042	0.027	0.002	0.011	57.137	0.196	0.4	56.923	0.208	4.8	449.5	1.4
3.3	4.2683	0.0001	0.0003	0.010	0.022	0.002	0.011	59.044	0.193	0.1	59.003	0.208	4.8	464.0	1.4
3.5*	9.9467	0.0001	0.0001	0.009	0.010	0.001	0.011	59.248	0.206	0.1	59.216	0.211	11.2	465.5	1.5
3.7	6.1767	0.0003	0.0002	0.029	0.019	0.002	0.011	57.905	0.168	0.2	57.818	0.177	7.0	455.8	1.2
3.9	1.7667	0.0004	0.0006	0.060	0.054	0.001	0.011	54.969	0.233	0.2	54.852	0.296	2.0	434.9	2.1
4.6*	23.4385	0.0004	0.0001	0.114	0.014	0.002	0.011	59.468	0.169	0.2	59.337	0.173	26.5	466.3	1.2
5.0	0.9415	0.0005	0.0018	0.096	0.113	0.001	0.011	55.981	0.543	0.2	55.845	0.751	1.1	441.9	5.2
5.5	0.6713	0.0024	0.0012	0.133	0.153	0.004	0.011	55.982	0.391	1.2	55.287	0.533	0.8	438.0	3.7
6.5	0.4256	0.0059	0.0020	0.256	0.256	0.002	0.011	55.695	0.528	3.1	53.941	0.790	0.5	428.5	5.6
15.0*	6.4141	0.0010	0.0001	0.098	0.020	0.003	0.011	59.772	0.134	0.5	59.477	0.139	7.2	467.3	1.0

(continued)

Table 1. Laser step-heating ^{40}Ar/^{39}Ar data *(continued)*

Power[a]	Vol. ^{39}Ar x10^{-11} cc	^{36}Ar/^{39}Ar	±	^{37}Ar/^{39}Ar	±	^{38}Ar/^{39}Ar	±	^{40}Ar/^{39}Ar	±	%^{40}Ar ATM	*^{40}Ar/^{39}Ar	±	f$_{39}$[b] (%)	Apparent Age (Ma[c])	±
07SNB-S165A-02 Amphibole; J=.00493160[d] (Z9607; 50.051611°N 56.107472°E)															
									Aliquot: 1						
2.6*	0.0264	0.0524	0.0532	3.455	4.739	0.299	0.050	77.011	6.881	20.1	61.535	16.837	1.6	481.5	115.0
3.0*	0.0150	0.0475	0.0846	1.190	6.793	0.043	0.115	94.634	8.175	14.8	80.610	26.169	0.9	608.3	166.7
3.9*	0.5158	0.0005	0.0039	0.606	0.235	-0.006	0.011	59.012	0.919	0.2	58.878	1.462	30.2	463.1	10.1
4.4	0.2311	0.0022	0.0067	0.807	0.457	-0.006	-0.013	55.968	0.880	1.2	55.322	2.174	13.6	438.3	15.2
4.8*	0.5441	0.0015	0.0033	14.256	0.515	0.079	0.012	59.898	0.671	0.7	59.462	1.192	31.9	467.2	8.2
5.0*	0.1433	0.0010	0.0113	48.271	1.830	0.117	0.016	60.378	1.411	0.5	60.090	3.617	8.4	471.5	24.8
5.5*	0.0303	-0.0096	-0.0426	37.057	3.815	0.003	0.026	62.045	3.688	-4.6	64.892	13.143	1.8	504.5	88.6
6.5*	0.0612	0.0029	0.0191	30.428	3.116	0.018	0.018	59.619	2.709	1.4	58.772	6.247	3.6	462.4	43.1
8.0*	0.0576	-0.0005	-0.0169	19.622	2.015	-0.007	-0.024	57.381	2.726	-0.2	57.515	5.689	3.4	453.6	39.4
15.0*	0.0811	0.0005	0.0189	28.689	2.428	0.085	0.028	61.916	2.701	0.3	61.758	6.204	4.8	483.0	42.3
07SNB-S170A-01 Muscovite; J=.00492940[d] (Z9610; 50.05875°N 56.119722°E)															
									Aliquot: 1						
2.6	1.9017	0.0007	0.0010	0.001	0.007	0.003	0.011	53.012	0.446	0.4	52.814	0.536	3.8	420.3	3.8
2.8	1.6582	0.0003	0.0009	0.005	0.008	-0.001	-0.011	52.935	0.322	0.2	52.853	0.408	3.3	420.6	2.9
3.0*	4.6804	0.0003	0.0003	0.005	0.003	0.002	0.011	53.528	0.180	0.2	53.437	0.200	9.3	424.8	1.4
3.3*	2.1296	0.0004	0.0006	0.006	0.007	0.002	0.011	53.448	0.228	0.2	53.318	0.291	4.2	423.9	2.1
3.5*	4.2070	0.0006	0.0003	0.006	0.004	0.002	0.011	53.636	0.146	0.3	53.448	0.173	8.3	424.8	1.2
3.7*	2.6770	0.0008	0.0005	0.007	0.005	0.001	0.011	53.693	0.244	0.4	53.459	0.287	5.3	424.9	2.0
3.9*	4.6679	0.0002	0.0003	0.001	0.003	0.001	0.011	53.602	0.154	0.1	53.531	0.177	9.2	425.4	1.3
4.2*	4.8455	0.0008	0.0003	0.003	0.003	0.002	0.011	53.801	0.154	0.4	53.566	0.175	9.6	425.7	1.2
4.6*	6.5205	0.0009	0.0002	0.003	0.002	0.002	0.011	53.805	0.173	0.5	53.529	0.184	12.9	425.4	1.3
5.5*	6.8980	0.0000	0.0002	0.002	0.002	0.002	0.011	53.515	0.189	0.0	53.509	0.200	13.6	425.3	1.4
6.0*	1.6170	0.0004	0.0006	0.002	0.006	0.001	0.011	53.554	0.268	0.2	53.423	0.317	3.2	424.7	2.2
6.5	1.1850	0.0005	0.0010	0.001	0.010	0.000	-0.011	52.706	0.293	0.3	52.567	0.419	2.3	418.6	3.0
15.0	7.5790	0.0010	0.0002	0.001	0.002	0.002	0.011	54.346	0.142	0.6	54.046	0.157	15.0	429.1	1.1
08SNBY113B1 Amphibole; J=.00440900[e] (Z9760; 50.046083°N 56.110583°E)															
									Aliquot: 1						
3.0	0.0062	1.6826	0.4266	6.712	2.426	2.334	0.545	1158.768	251.568	42.9	661.551	161.610	0.8	2487.6	329.6
3.5*	0.0061	0.0418	0.2148	1.167	1.354	0.082	0.215	75.407	43.987	16.4	63.067	74.823	0.7	445.7	466.9
3.9*	0.0138	0.1010	0.0898	4.591	1.041	0.113	0.049	100.858	19.760	29.6	71.021	32.159	1.7	494.9	194.9
4.2*	0.0829	0.0611	0.0152	13.992	0.341	0.468	0.024	82.270	3.128	21.9	64.230	5.403	10.1	453.0	33.5
4.6*	0.2324	0.0085	0.0102	51.288	1.129	1.576	0.041	67.447	1.777	3.7	64.922	3.480	28.3	457.3	21.5
5.0*	0.0867	0.0475	0.0205	84.037	1.052	1.463	0.045	84.581	2.890	16.6	70.541	6.692	10.6	492.0	40.6
5.5*	0.2010	0.0259	0.0178	98.216	1.994	2.206	0.051	72.062	1.855	10.6	64.421	5.531	24.5	454.2	34.3
6.0*	0.0303	0.0365	0.0452	107.577	8.621	2.138	0.182	77.976	10.033	13.8	67.180	16.366	3.7	471.3	100.5
15.0*	0.1614	0.0268	0.0226	120.062	2.297	2.803	0.065	72.872	1.999	10.9	64.960	6.930	19.7	457.6	42.9
08SNBT127A1 Amphibole; J=.00441210[e] (Z9761; 49.930306°N 56.2055°E)															
									Aliquot: 1						
3.2*	0.0040	4.0406	1.2597	33.224	9.847	1.778	0.580	1305.175	383.433	91.5	111.188	142.356	0.5	725.5	768.4
3.9*	0.0462	0.2700	0.0359	24.683	0.858	0.203	0.019	144.864	6.179	55.1	65.080	11.186	5.2	458.6	69.2
4.6*	0.6012	0.0209	0.0040	21.811	0.286	0.247	0.015	70.255	0.913	8.8	64.086	1.459	67.8	452.4	9.1
5.0*	0.0525	0.0088	0.0177	26.920	0.707	0.386	0.031	68.536	3.862	3.8	65.925	6.492	5.9	463.9	40.0
5.5*	0.0238	0.0142	0.0376	31.564	1.742	0.353	0.030	69.257	8.416	6.1	65.067	13.862	2.7	458.5	85.7
6.0*	0.0352	0.0037	0.0243	43.674	1.518	0.432	0.024	69.274	5.553	1.6	68.194	9.052	4.0	477.9	55.4
15.0*	0.1245	0.0087	0.0126	42.360	0.914	0.374	0.023	66.518	1.967	3.9	63.954	4.187	14.0	451.6	26.0
08SNBT130A1 Amphibole; J=.00439890[e] (Z9762; 49.6265°N 56.45375°E)															
									Aliquot: 1						
3.0*	0.0893	0.2946	0.0278	3.161	0.191	0.142	0.017	150.074	7.067	58.0	63.019	8.120	1.5	444.5	50.5
3.9*	0.1542	0.0662	0.0087	2.849	0.075	0.017	0.013	82.834	1.964	23.6	63.267	3.073	2.5	446.1	19.1
4.6*	0.4459	0.0071	0.0032	4.301	0.056	0.029	0.011	63.749	0.741	3.3	61.664	1.189	7.3	436.0	7.4
5.0*	0.6696	-0.0005	-0.0030	7.485	0.079	0.066	0.011	62.596	0.596	-0.2	62.741	1.080	11.0	442.8	6.7
5.5*	1.8860	0.0028	0.0018	8.328	0.056	0.076	0.011	63.246	0.319	1.3	62.417	0.607	31.0	440.7	3.8
6.0*	1.4241	0.0035	0.0018	7.712	0.118	0.078	0.011	63.088	0.849	1.6	62.051	0.993	23.4	438.4	6.2
15.0*	1.4098	0.0048	0.0027	10.717	0.107	0.077	0.011	63.598	0.569	2.2	62.191	0.961	23.2	439.3	6.0

[a]: As measured by laser in % of full nominal power (10W)

[b]: Fraction 39Ar as percent of total run (where two aliquots were analyzed, gas is normalized to total ^{39}Ar of both aliquots)

[c]: Errors are analytical only and do not reflect error in irradiation parameter J

[d]: Nominal J (0.3% 1σ error), from GSC Irradiation Batch #57, referenced to FCT-San = 28.201 ± 0.023 Ma (1σ, Kuiper et al. 2008)

[e]: Nominal J (0.3% 1σ error), from GSC Irradiation Batch #58, referenced to FCT-San = 28.201 ± 0.023 Ma (1σ, Kuiper et al. 2008)

[f]: Blanks were measured before and after aliquot analysis and levels varied between ^{40}Ar =1.8*10-7 to 5.3*10-7 nmol, ^{39}Ar = 7.8*10-10 to 3.9*10-9 nmol, ^{38}Ar = 4.9*10-10 to 1.6*10-9 nmol, ^{37}Ar =2.3*10-9 to 6.2*10-9 nmol, ^{36}Ar = 5.6*10-10 to 4.1*10-9 nmol, all at ± 20% uncertainty (2σ). Nucleogenic interference corrections are (^{40}Ar/^{39}Ar)K = 0.025±.005, (^{38}Ar/^{39}Ar)K = 0.011±0.010, (^{40}Ar/^{37}Ar)Ca = 0.002±0.002, (^{39}Ar/^{37}Ar)Ca = 0.00068±0.00004, (^{38}Ar/^{37}Ar)Ca = 0.00003±0.00003, (^{36}Ar/^{37}Ar)Ca = 0.00028±0.00016

*Laser steps marked with an asterisk denote those used in the plateau or pseudo-plateau age calculation

All errors reported at the 2σ level of incertainty, unless otherwise indicated

Decay Constant (^{40}K λtotal) = 5.463 (± 0.107) x 10^{-10}/yr (Min et al. 2000)

are assumed to pass through the $^{40}Ar/^{36}Ar$ value for atmospheric air (295.5). Blank levels and nucleogenic interference correction values are stated in Table 1. One aliquot was analyzed for each sample initially. In cases where the spectrum from the first aliquot was inconclusive, a second aliquot was then carried out. In gas release diagrams, multiple step-heating analyses are combined to form a single result, whereby the fraction of ^{39}Ar released relative to the sum total of ^{39}Ar released for all analyses forms the x-axis. Thus, the apparent $^{40}Ar/^{39}Ar$ age of each heating step is plotted against the cumulative amount of ^{39}Ar released from the sample, normalized to 100% for the total ^{39}Ar released over all aliquots. Because of the use of replicate aliquots, some of the gas release plots presented here differ from conventional $^{40}Ar/^{39}Ar$ spectra in that data from each aliquot is displayed in adjacent, alternately shaded regions of a gas release spectrum. Upon ascertaining reproducibility of individual spectra and plateau regions between aliquots, data were combined by integrating plateau portions (defined as three or more consecutive heating steps that comprise greater than 50% of the total ^{39}Ar released, marked by black steps in age spectra) weighted by analytical error. Errors reported in the text and table are at the 2σ uncertainty level, unless otherwise indicated. Errors on the plateau ages include both analytical error and error in the J-factor, but not error in the decay constants. Incorporation of the ^{40}K decay constant error increases the $^{40}Ar/^{39}Ar$ plateau age errors to approximately 4% (2σ).

U–Pb Geochronology and Trace Element Geochemistry

Due to the extremely fine grain size (<25 μm) of the zircon grains in the amphibolitized eclogite sample (SNB-06-020), employing standard mineral separation techniques and U–Pb dating of the zircon using conventional ID–TIMS was considered impractical. Instead, the zircon grains from rock chips and thin section fragments were prepared for *in situ* analysis by following the procedures outlined in Rayner and Stern (2002). Prior to *in situ* U–Pb analysis by Sensitive High Resolution

Ion Microprobe (SHRIMP), the locations of zircon grains in several polished thin sections and polished thin section off-cuts were identified using an automated scanning routine on a Zeiss EVO 50 series scanning electron microscope (SEM) at the Geological Survey of Canada (GSC) in Ottawa. The beam was operated at 20 kV accelerating voltage and 500 pA current. Areas of the thin sections and rock fragments containing the largest viable grains were then drilled out and the cores were cast in a 2.5 cm diameter epoxy mount (GSC IP477) along with fragments of the GSC laboratory standard zircon (z6266, with $^{206}Pb/^{238}U$ age = 559 Ma) and the Temora-2 zircon secondary standard ($^{206}Pb/^{238}U$ = 416.8 +/–0.33 Ma (2σ); Black et al. 2004). *In situ* zircon grains were then imaged again with the same SEM in both back-scattered electron (BSE) and cathodoluminescence (CL) mode to provide insight into their petrographic context, identify internal zoning, cracks and mineral inclusions, and to guide analytical spot placement. The mount surface was evaporatively coated with 10 nm of high purity Au. Analytical procedures and calibration details for the SHRIMP II at the GSC followed those described by Stern (1997) and Stern and Amelin (2003). Analyses were conducted using a $^{16}O^-$ primary beam, projected onto the zircon grains at 10 kV. Prior to analysis, the ion beam was rastered over the area of interest for 3 minutes in order to remove the Au coating locally and eliminate effects of surface common lead. The sputtered area used for analysis was ca. 7 x 9 μm with a beam current ranging between 0.7 and 1.0 nA. Count rates were sequentially measured over 6 scans with a single electron multiplier and a pulse-counting system with deadtime of 23 ns. The results presented here were obtained during two consecutive analytical sessions under similar analytical conditions. Details of the analytical conditions are presented in the footnotes of the data tables. Off-line data processing was accomplished using the LEAD and PRAWN data reduction programs of T.R. Ireland (unpublished program routine). The 1s external errors of $^{206}Pb/^{238}U$ ratios reported in the data table incorporate a ± 1.3 % error in

calibrating the standard z6266 zircon. Analyses of the secondary zircon standard, Temora-2, were interspersed between the sample analyses to verify the accuracy of the U–Pb calibration. Using the calibration defined by the z6266 standard, the weighted mean $^{206}Pb/^{238}U$ age of 11 SHRIMP analyses of Temora-2 zircon was 418.9 ± 5.6 Ma (95% conf.). Isoplot v. 3.00 (Ludwig 2003) was used to calculate the $^{206}Pb/^{238}U$ apparent ages in U–Pb data Table 2 and to generate the Tera-Wasserburg plot. Errors for isotopic ratios and apparent ages in Table 2 are given at 1s uncertainty. Error ellipses and the lower intercept age error are reported at 2σ. Age errors reported in the text are at the 2σ uncertainty level. No fractionation correction was applied to the Pb-isotope data.

Trace element analyses of zircon were carried out by SHRIMP during a separate analytical session. Analyses were done in the same grains and pits as the U–Pb runs, where possible, using the same 7 x 9 μm spot size. Twenty isotopic species were collected, including all the lanthanides, Y, Ba, Ta, Hf, Th and U, the count rates for which were measured sequentially over 4 scans. Abundances were calibrated against zircon standard z6266 that is chemically homogeneous at the micrometre scale (Stern 2001). External uncertainties relating to the standard composition determined by inductively coupled plasma mass spectrometry (2–5%, unpublished data) are not included. Uncertainties associated with the measurements of the light rare earth elements (LREE; La to Nd), in particular, are large due, in part, to the small analytical spot size. For this reason, they will not be discussed further here. Measurement and calibration errors on abundances for middle rare earth elements (MREE) to heavy rare earth (HREE; Sm to Lu) are typically between 5–20% (1σ) with the exception of Sm (50–60% for Type I, >96% for Type II), Eu (51–89%), Er (15–61% for Type I), Gd (40–55% for Type II), and Tm (15–67% for Type II).

$^{40}Ar/^{39}Ar$ Data

Samples for $^{40}Ar/^{39}Ar$ analyses were taken from three lithotectonic units: the Birchy Complex, the Advocate

Table 2: SHRIMP U–Pb analytical data for Type I zircon

SNB-06-020 (lab# Z9536) Fleur-de-Lys gabbro, 49.80531° N, 56.40817°W

Spot name	U (ppm)	Th (ppm)	$\frac{Th}{U}$	$\frac{^{204}Pb}{^{206}Pb}$	±	$\frac{^{208*}Pb}{^{206*}Pb}$	±	$\frac{^{206*}Pb}{^{238}U}$	±	$\frac{^{207*}Pb}{^{206*}Pb}$	±	Age (Ma)*** $\frac{^{206}Pb}{^{238}U}$	±	Host
9536-133.1	82	35	0.442	0.00356	0.00225	0.54580	0.11492	0.08172	0.00405	0.15320	0.00922	448	22	Interstitial btw grt grains
9536-133.2**	58	23	0.40053	0.00892	0.00300	0.25339	0.08464	0.07426	0.00593	0.15077	0.01286	409	33	
9536-188.2	1861	2304	1.27878	0.00004	0.00007	0.42420	0.01212	0.07725	0.00165	0.06186	0.00089	477	10	Along contact btw qtz, fsp, amph
9536-311.1	277	187	0.69692	0.00001	0.00001	0.23152	0.02629	0.07872	0.00140	0.06663	0.00285	483	9	
9536-311.2	312	533	1.76258	0.00214	0.00081	0.90057	0.06176	0.07935	0.00136	0.08390	0.00577	476	9	Entirely within amphibole
9536-311.1.2	350	196	0.57757	0.00001	0.00001	0.24668	0.03838	0.07511	0.00143	0.07722	0.00675	455	9	
9536-311.2.2	255	231	0.93459	0.00313	0.00099	0.47582	0.04035	0.07349	0.00261	0.08983	0.00457	439	15	
9536-380.1	206	87	0.43678	0.00312	0.00199	0.15466	0.04037	0.07348	0.00257	0.07167	0.00406	449	16	fsp-grt-qtz matrix
9536-560.1**	44	50	1.17658	0.00001	0.00001	0.50115	0.12020	0.07503	0.00409	0.09979	0.00909	442	24	fsp-amph-qtz matrix
9536-944.1	225	52	0.23665	0.00154	0.00067	0.09815	0.01860	0.07358	0.00158	0.07629	0.00651	447	10	fsp-amph-qtz matrix

Mount IP477, K50 spot size, primary intensity ~0.8nA

Spot name follows the convention x-y:z; where x = sample number, y = grain number and z = spot number. Multiple analyses in an individual spot are labelled as x-y:z.z

Uncertainties reported at 1s and are calculated by numerical propagation of all known sources of error

* refers to radiogenic Pb (uncorrected for common Pb)

**Indicates an analysis for which the ion beam appears to have hit both Type I core and Type II overgrowth

Calibration standard 6266; U = 910 ppm; Age = 559 Ma; $^{206}Pb/^{238}U$ = 0.09059

Error in $^{206}Pb/^{238}U$ calibration 1.30%

Th/U calibration: F = 0.03900*UO + 0.85600

***^{207}Pb-Corrected ages were calculated using the ^{207}Pb-method; Stacey and Kramers (1975) model common Pb composition (t = age of zircon) was used

btw: between, fsp: feldspar, qtz: quartz, amph: amphibole, grt: garnet

Complex, and a sample from the East Pond Metamorphic Suite, south of Wild Cove Pond (Figs. 1 and 2).

Birchy Complex
Four samples come from three localities of the Birchy Complex in the vicinity of Coachman's Cove (Fig. 2). At the first locality, three phases of deformation are readily distinguished: open upright F_3 folds overprinting isoclinal F_2 and an axial planar S_2 crenulation foliation, which affects a penetrative S_1 differentiated metamorphic layering (Fig. 3A; Bursnall 1975). Both amphibole and white mica were extracted from a sample of epidote- and hornblende-bearing mafic schist (07-SNB-S165) complexly interlayered structurally with psammite, coticule and metagabbroic layers. The white mica could be derived from a quartz veinlet (Fig. 3B) or a thin interlayered psammitic band. One aliquot of amphibole (3 grains, 500–800 μm each) was analyzed and gave a plateau age of 466.4 ± 6.5 Ma (MSWD=0.729; Fig. 4A), yielding a mid-temperature dropout step and variable Ca/K ratios. Two aliquots of muscovite were analyzed; both the first (4 thin colourless grains, 400–600 μm each) and second aliquots (3 thick pale yellow grains, 500–700 μm each) yielded similar spectra with small, medium and high temperature dropout steps that gave a combined plateau age of 466.9 ± 2.5 Ma (MSWD = 1.422; Fig. 4B).

The second locality is from a coastal exposure south of Coachman's Cove. Here, interlayered medium-grained, intensely folded (same three phases as above) metabasaltic or mafic volcaniclastic rock with coticule is interlayered with pegmatitic gabbro. Amphibole was extracted from the gabbro (08-SNB-Y113) and a single aliquot was analyzed (2 large grains; Fig. 3C). It yielded a plateau age of 460.5 ± 14.2 Ma (MSWD = 0.420; Fig. 4C).

The third sample was collected from the western shoreline of the cove where strongly sheared psammite (07-SNB-S170) and mafic schist are exposed just south of the faulted contact with the Rattling Brook Group (Pardee fault; Fig. 2). In this locality, D_2 strain is more intense and the main foliation is a composite S_{1-2} fabric (Fig.

3D), that is in turn folded by F₃. A muscovite aliquot (2 thin pale yellow grains, 800 and 1100 μm) separated from the psammite yielded a plateau age of 425.1 ± 2.3 Ma (MSWD = 0.414; Fig. 4D). The fusion step, not included in the plateau, gave an apparent age of ca. 429 Ma.

Advocate Complex

Three samples were taken from a unit of metagabbro and mafic schist of the Advocate Complex. The sampled rocks are structurally sandwiched between the serpentinized ultramafic rocks of the Advocate Asbestos mine (Fig. 5A; part of hanging wall Duck Island Cove sequence of Bursnall 1975) and zoisite-altered leucogabbro and associated mafic rocks (Marble Cove sequence of Bursnall 1975) in the footwall. This shear zone also comprises narrow tectonic slices of highly strained, zoisite-altered anorthositic gabbro, black graphitic pelite and intensely serpentinized peridotite. Sample 06SNB-S085 is a fine-grained epidote-plagioclase amphibolitic gabbro (ca. 483 Ma U–Pb zircon crystallization age; V. McNicoll personal communication 2009). The U/Pb age of this rock is younger than available ages for the BVOT (489–487 Ma) and may be contemporaneous with early tholeiitic mafic magmatism in the ophiolite cover sequence (e.g. 483 +8.7/–4.8 Ma Stog'er Tight gabbro, Ramezani 1993). The geochemistry of this metagabbro reveals that it is tholeiitic, has modest enrichment in TiO₂ (1.3 wt.%) and has a chondrite-normalized LREE-enriched profile. These chemical features are in stark contrast to Advocate Complex intrusive rocks that have boninitic affinities, or to late tholeiitic gabbro in the ophiolite that is LREE-depleted, but is similar to gabbro and related mafic volcanic rocks in the ophiolite cover sequence. We interpret this sample to represent a tectonic slice of early erupted ophiolite cover that has been imbricated with the lower part of the obducted ophiolite. Only one penetrative fabric was noted, which may represent a composite S_{1-2}. In thin section, sub-millimetric amphibole grains are fractured and contain inclusions and vary in colour from medium greyish-green to bluish-green (Fig. 5B). One aliquot (2 large dark greyish-green
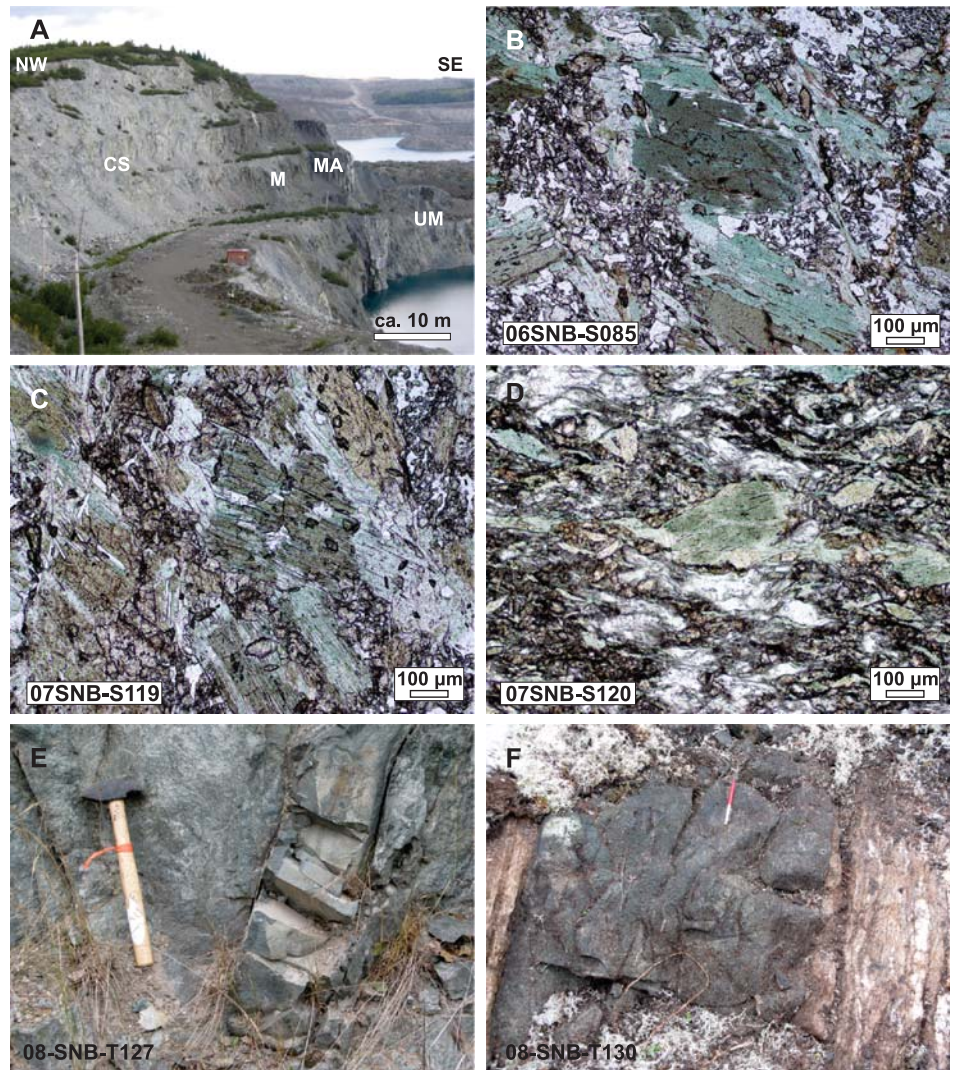
Figure 5. Photographs of dated Advocate Complex (A–E) and East Pond Metamorphic Suite (F) localities and thin sections. A: Oblique view of the northwestern wall of southwestern part of the Advocate mine. CS: calc-silicate-altered gabbro; M: mafic schist and amphibolitic gabbro; MA: mylonitic schist and amphibolite; UM: serpentinized ultramafic units. B–D: Photomicrograph (plane-polarized light) of thin sections showing typical amphibole porphyroblasts from localities 06SNB-S085(B), 07SNB-S119 (C) and 07SNB-S119 (D). E–F: photographs of sampled lithologies from localities 08SNB-T127 Advocate gabbro (E) and 08-SNB-T130 amphibolite (F). See Figures 1 and 2 for sample locations.

grains, 700 and 1000 μm) yielded a fairly flat plateau at 465.1 ± 4.3 Ma (MSWD = 0.701), with fairly stable Ca/K ratios (Fig. 6A).

A similar medium-grained epidote-plagioclase amphibole-rich gabbro (sample 07SNB-S119: Fig. 5C), was taken ca. 10 m away from the previous sample. Two amphibole aliquots were analyzed, however only one gave an interpretable result (4 pale greyish-green grains, 300–600 μm each). It yielded a plateau age of 470.2 ± 3.5 Ma (MSWD = 0.581), with slightly

ascending Ca/K ratios (Fig. 6B). The low-temperature pseudo-plateau, representing 19% of the ^{39}Ar gas, gave an age of 457.5 ± 5.5 Ma (MSWD = 0.168) and low Ca/K ratios, which may represent microscopic biotite intergrowths, a more K-rich phase of amphibole or the maximum age of a recrystallization or resetting event.

The third sample 07SNB-S120 was taken ca. 325 m to the northeast of the other samples, from an exposure of mafic schist. Only one fabric was observed in outcrop, although
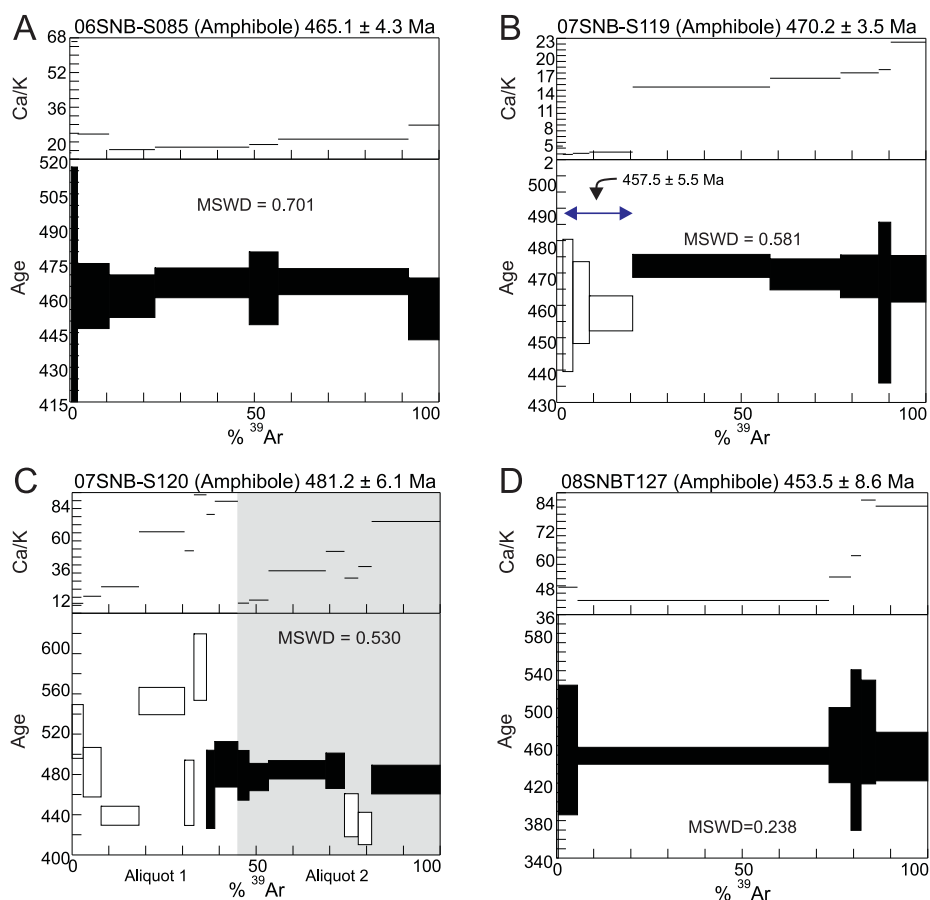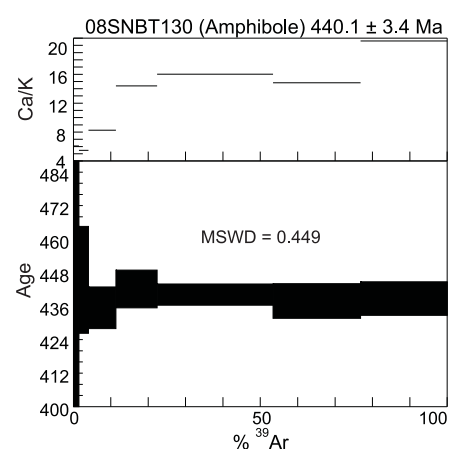
Figure 6. ^{40}Ar/^{39}Ar step-heating spectra (all steps are presented at 2σ relative uncertainties) and ^{37}Ar$_{Ca}$/^{39}Ar$_K$ ratio diagrams of Advocate Complex samples. Plateau segments are shown in black. Plateau age uncertainties are 2σ and include both analytical and J-factor errors. A: Amphibole aliquot from sample 06SNB-S085. B: Amphibole aliquot from sample 07SNB-S119. C: Combined amphibole aliquots from sample 07SNB-S120. D: Amphibole aliquot from sample 08SNB-T127. See Figures 1 and 2 for sample locations. MSWD: mean square of weighted deviates.

Figure 7. ^{40}Ar/^{39}Ar step-heating spectrum (all steps are presented at 2σ relative uncertainties) and ^{37}Ar$_{Ca}$/^{39}Ar$_K$ ratio diagram of East Pond Metamorphic Suite amphibolite sample 08-SNB-T130. Plateau age uncertainty is 2σ and includes both analytical and J-factor error. See Figure 1 for sample location. MSWD: mean square of weighted deviates.

microscopic evidence suggests that it may represent a composite foliation (Fig. 5D). Two aliquots were analyzed (respectively 2 and 3 greyish-green polycrystalline amphibole grains, 400–700 μm each). The first gave a very disturbed age spectrum and Ca/K plot, with high Ca/K values. The second aliquot was less disturbed, and yielded a quasi-plateau age with two mid-temperature dropout steps, which, if combined with the concordant high-temperature steps of the first aliquot, provides an age of 481.2 ± 6.1 Ma (MSWD = 0.530; Fig. 6C). The poly-crystalline nature of the grains, possibly containing small intergrowths with other mineral phases, the degassing of which may have caused the scatter in the Ca/K plots and age spectrum,

including the two dropout steps of aliquot #2. Alternatively, the latter may reflect an isotopic disturbance at ca. 430 Ma.

A fourth sample (08SNB-T127A-01) comes from a shoreline locality of coarse-grained gabbro in the town of Baie Verte (Fig. 5E). In thin section, amphibole is sub-millimetric, pale green, with brownish rims, fractured and contains numerous inclusions. One amphibole aliquot (2 grains) was analyzed and, despite elevated and irregular Ca/K ratios, yielded a plateau age of 453.5 ± 8.6 Ma (MSWD = 0.238; Fig. 6D). This age was weighted primarily on the third heating step, which comprised 68% of the total released ^{39}Ar, and gave an apparent age of 452 Ma. The highest temperature

steps were volumetrically smaller and gave relatively imprecise ages between 452 and 478 Ma.

East Pond Metamorphic Suite
Amphibole was extracted from a layer of amphibolite (08SNB-T130) within medium-grained psammite of the East Pond Metamorphic Suite northwest of Micmac Lake. The amphibolite occurs as a 40 cm wide layer that is concordant with the main foliation (Fig. 5F), which is interpreted as the regional S$_2$ fabric, although proximity with an interpreted D$_4$ shear zone associated with the Baie Verte Road fault system is noteworthy (Fig. 1). One aliquot consisting of two polycrystalline grains of amphibole was analyzed and yielded a plateau age of 440.1 ± 3.4 Ma, with staircase ascending Ca/K ratios as high as 23 (Fig. 7).

Zircon U–Pb Data and Trace Element Geochemistry
A partly retrogressed eclogite locality (SNB-06-020) of the East Pond Metamorphic Suite was sampled on the north shore of Gull Pond (Figs. 1 and 3E). The sample comes from a site described by Church (1969), and later studied by Jamieson (1990), who conducted petrography, mineralogy and
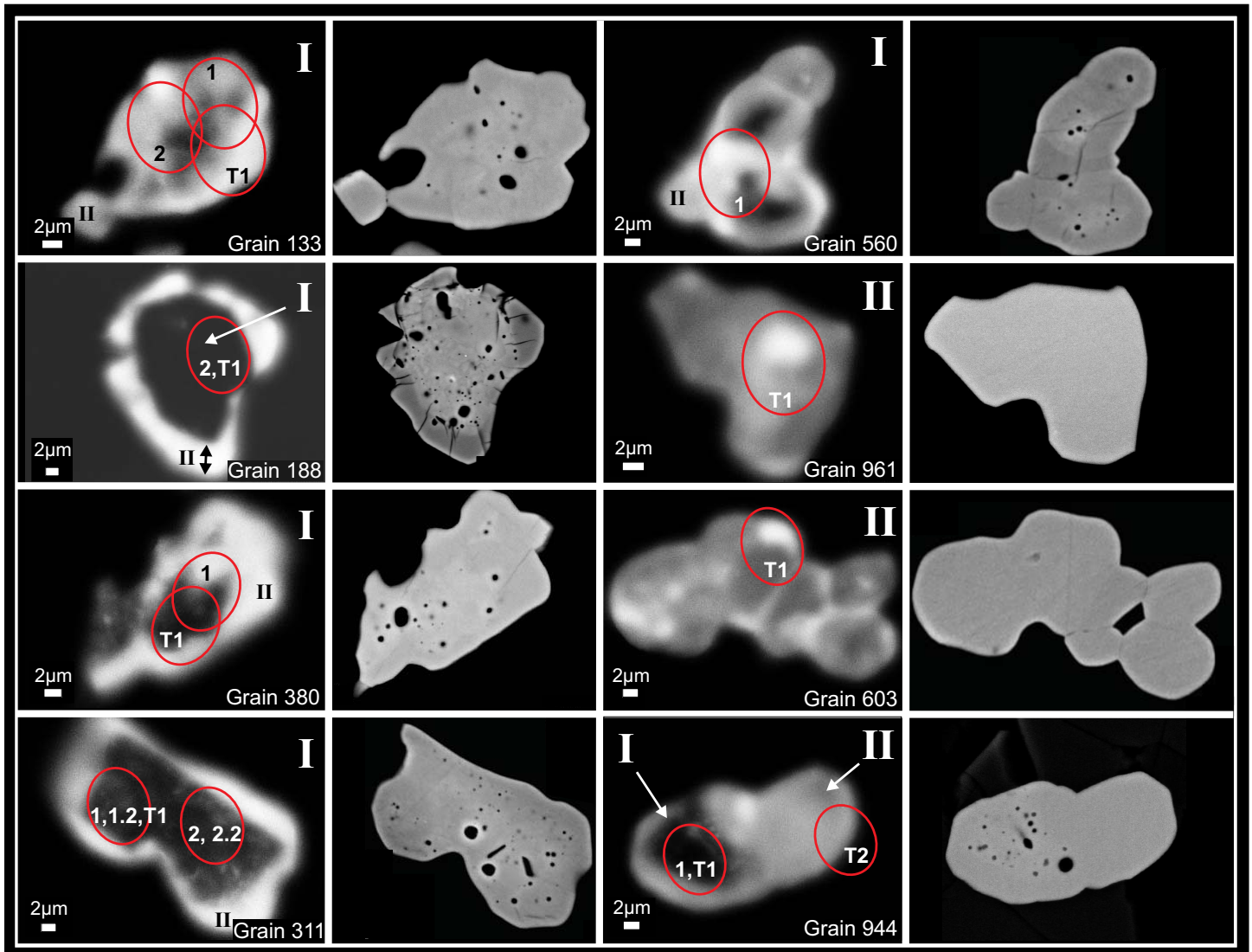
Figure 8. Cathodoluminescence (CL) and back-scattered electron image pairs for zircon grains analyzed for U–Pb and trace elements on the SHRIMP. Resolution on the CL images (left side of each pair) is poor due to the extremely small grain sizes of the zircon. U–Pb analysis spots are numbered 1, 2, 3, etc., while trace element spots are labelled with T1 or T2.

P–T work on the eclogite. The sample site comprises a tabular body (~1 m wide) of metagabbro with a pale green weathering (pyroxene) fine- to medium-grained eclogitic core enveloped in a thicker, dark green garnet amphibolite. Our sample was collected near the margin of the body. Early metamorphism of this sample is represented by clinopyroxene (omphacite?) + white mica (phengite?) + rutile ± rare garnet and is equivalent to the early eclogitic metamorphic paragenesis of Jamieson (1990). The main retrogressive amphibolite assemblage consists of hornblende + garnet + zoisite + plagioclase + epidote and is the same as the main amphibolitic assemblage of Jamieson (1990). Clinopyroxene occurs as

anhedral, partly resorbed crystals charged with small inclusions (quartz + plagioclase?) and surrounded by relatively clear, large (up to 7 mm) later hornblende. Relict garnet forms as rare, large (2–3 mm) single anhedral grains engulfed by hornblende and late garnet. The majority of the garnet in the rock forms small idioblastic grains, polyhedral aggregates, and as chains of well-formed crystals that locally cut across hornblende, and are interpreted to be late-formed. Rutile, white mica, zoisite, and trace amounts of epidote and plagioclase form as well-formed crystals.

$^{40}Ar/^{39}Ar$ analyses of amphibole and white mica from this locality revealed the presence of an excess

argon component and did not provide interpretable data. Zircon grains in the sample are scarce, very small (<25 μm) and many occur along grain boundaries or at triple points, most commonly within domains dominated by hornblende, quartz, zoisite, rutile, and to a lesser extent, clinopyroxene and idioblastic garnet. Thin section examination and secondary electron microscope (SEM) imaging revealed two varieties of zircon, distinguished by their texture, cathodoluminescence (CL; Fig. 8), and geochemistry (see below). Type I zircon is anhedral, with irregular grain boundaries that are locally embayed. In CL, Type I zircon is dark grey to black (high in U), with no distinct zoning. Holes and inclu-

sions are common giving the mineral a spongy appearance. Most of the inclusions are round and bubble-shaped, and were identified using the SEM as epidote, hornblende, clinozoisite, quartz, plagioclase, clinopyroxene and thorite. In contrast to Type I grains, Type II zircon is inclusion-free, very bright in CL (much lower in U) and locally forms amalgamated groups of equant and multifaceted grains, or more commonly as overgrowths on inclusion-rich Type I cores.

Type II zircon rims were either not wide enough to accommodate an ion probe spot and/or did not contain sufficient U for meaningful U–Pb analyses (1–1.4 ppm U). Only nine Type I zircon grains were analyzed using the SHRIMP, of which six yielded analytically meaningful results. Two of the grains were analyzed more than once in order to confirm reproducibility of the U–Pb ages obtained from so few viable targets. Grain 133 accommodated two spots which were slightly overlapping. Two spots were analyzed on grain 311, with two analyses done in each pit (see Figure 8 for all analytical spot locations). Trace element concentrations in the Type I grains were analyzed in the same locations as the U–Pb spots. Type II grains and overgrowth domains on Type I zircon were also targeted to compare the trace element signature of the two zircon varieties. Each spot for U–Pb and trace element calibration was placed at a location on z6266 and/or Temora-2 zircon that had not been previously analyzed. Due to the exceedingly small grain size of the zircon grains, they were difficult to locate precisely in reflected light, and positioning the ion beam exactly on the desired spot in the grain was challenging for both the U–Pb and trace element analyses. For this reason, some of the spot locations were not ideal; some spots were partially off the grain (e.g. analyses 944.T2 and 603.T1 in Fig. 8), or the trace element and U–Pb spots were not exactly coincident (e.g. 133.1 and 133.T1 were intended to be in the same spot, as were 380.1 and 380.T1).

SHRIMP U–Pb Results
SHRIMP U–Pb results for Type I zircon are presented in Table 2 and are shown in a Tera-Wasserburg plot in
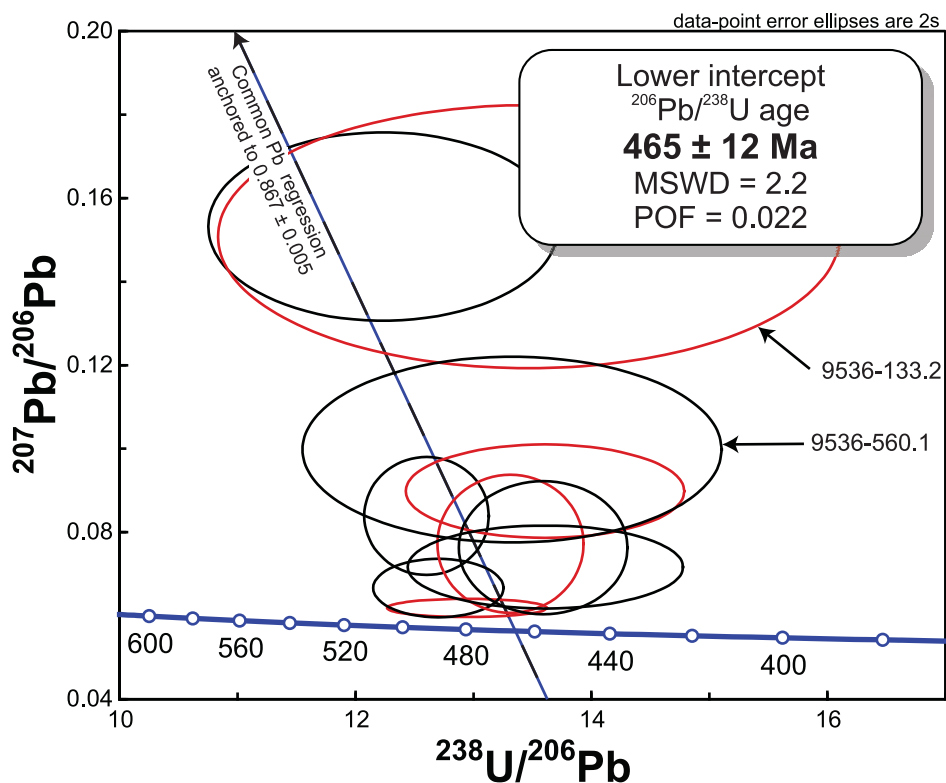
Figure 9. Tera–Wasserburg plot for sample SNB-06-020 showing isotopic data uncorrected for common Pb. Trend line shown is fitted through a Middle Ordovician common Pb isotopic composition (Stacey and Kramers 1975). Error ellipses represent 2σ level of uncertainty. Red ellipses are analyses that were done either slightly overlapping with or directly on top of a previously analyzed spot. The large error and slightly elevated mean square of weighted deviates (MSWD) of 2.2 is due in part to the small spot size and typically low levels of U and radiogenic Pb in the grains. POF: probability of fit.

Figure 9, in which the data fall broadly along a trend line anchored to the Mid Ordovician common $^{207}Pb/^{206}Pb$ isotopic composition (0.867 ± 0.005, Stacey and Kramers 1975). The lower intercept of this anchored regression gives a $^{206}Pb/^{238}U$ age of 465 ± 12 Ma, including all ten data points (replicate spots included). The large error and slightly elevated MSWD of 2.2 is due in part to the small spot size and typically low levels of U and radiogenic Pb in the grains. For analyses 9536-133.2 and 9536-560.1, the ion beam fell on both Type I and Type II material; however, the errors on both ages are larger than those for the other analyses, and both data points fall along the common Pb line from which the lower intercept age is calculated, and are, therefore included in the age calculation. Although the SHRIMP age is based on analyses from only six grains and the error is three times that which is normally achievable for zircon with

U concentrations between 44 and 1861 ppm, the results are considered meaningful.

Whole Rock and Trace Element Mineral Geochemistry Results
A whole rock analysis of the retrogressed eclogite sample (Table 3A) reveals that this rock is mafic (SiO_2 = 48.8, FeO_T = 12.7 and MgO = 7.69 wt.%), and has high FeO, TiO_2 and low K_2O abundances typical of low-K tholeiitic mafic rocks. The major element composition is similar to other eclogite and eclogitic-amphibolite dykes and boudinaged bodies intruding basement to the Fleur de Lys Supergroup (de Wit and Strong 1975). The chondrite-normalized REE profile (Fig. 10; analyses in Table 3B) of the whole rock is flat. In contrast, metagabbro and metabasalt in the Birchy Complex have light rare earth element (LREE) depleted profiles (van Staal et al. 2013).

Results from nine zircon SHRIMP trace element analyses are summarized in Table 3B and shown as chondrite-normalized REE plots in Figure 10. In general, Type I zircon exhibits a steeply sloping HREE profile, with significant enrichment of HREE relative to MREE, whereas Type II zircon has consistently lower abundances of HREE (Gd–Lu) and distinctly flatter HREE patterns. The following element comparisons between Type I and Type II zircon can be made, disregarding two analyses (560.T1 and 133.T1) that reflect a mix of compositions: Type II zircon is more depleted in Ta (0.3–1.2 ppm compared to 1.4–6.4 ppm in Type I), Y (13–86 ppm compared to 756–4866 ppm in Type I), Sm (0.03–0.1 ppm compared to 0.31–11.55 ppm in Type I), U (0.1–1.5 ppm compared 85.5–2335 ppm in Type I,), Th (0.03–0.24 ppm compared to 16.13–2569 ppm in Type I) and more enriched in Hf (12459–13236 ppm compared to 4698–6879 ppm in Type I). The most REE-rich Type I zircon (188.T1; Fig. 10) has a significant negative Eu anomaly, whereas the remaining Type I and Type II zircon categories have either no Eu anomaly or in the case one Type II zircon, a slightly positive Eu anomaly (603.T1). A number of both zircon types have positive Ce anomalies (Fig. 10). Type I zircon has Th/U values that range from 0.19 to 1.1, whereas Type II zircon has values of 0.017 to 1.6.

Interpretation of Data
$^{40}Ar/^{39}Ar$ Ages

Other than a few exceptions presented above and discussed below, the majority of analyzed samples from the Birchy and Advocate complexes yielded Ordovician ages. Considering the estimated peak temperatures associated with M_1 metamorphism (ca. 450–500°C; Jamieson 1990; Jamieson and O'Beirne-Ryan 1991), and adopting conservative Ar closing temperatures of 400 ± 50°C and 550 ± 50°C for white mica and amphibole, respectively (Dahl 1996; Villa 1998; Harrison et al. 2009), analyses presented above may be interpreted as reflecting cooling ages (white mica) or crystallization ages at or shortly following metamorphic peak (for amphibole).
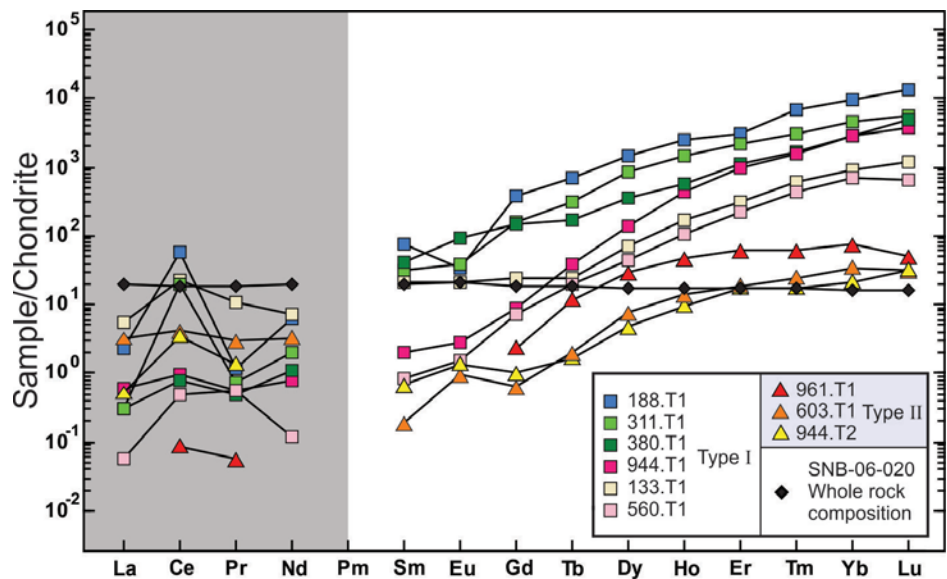
Figure 10. Trace element plot for Type I and Type II zircon grains and whole rock of the East Pond Metamorphic Suite amphibolitized eclogite (sample SNB-06-020), with chondrite normalizations following Sun and McDonough (1989). Grain numbers in the legend correspond to those in Table 3B that have the prefix *9536-*. Gaps in the data trends reflect measurements that were below detection limits. The LREE analyses in the grey portion of the plot are close to the detection limits and are not used for the purpose of the REE data interpretation.

The Birchy Complex locally preserves a relatively complete record of polyphase deformation (van Staal et al. 2103; Fig. 4). At least three generations of fabric development can be easily separated. The D_1 fabric is surprisingly well preserved and locally even represents the dominant schistosity. This is in contrast to highly strained rocks in areas near block-bounding shear zones. $^{40}Ar/^{39}Ar$ analyses from these relatively low strain windows (07SNB-S165 and 08SNB-Y113) gave slightly disturbed, but concordant results, within error, of ca. 466 Ma. Field and petrographic observations coupled with the nearly identical amphibole and muscovite ages suggest rapid post-metamorphic cooling, shortly following growth during M_1. At locality 07SNB-S170, the S_2 fabric is the most penetrative and dominant schistosity in the psammite, suggesting that the nearby D_1 Pardee fault (Kennedy 1971) was reactivated during D_2. Hence, the S_2 muscovite age of 425.1 ± 2.3 Ma probably represents cooling and/or penetrative recrystallization associated with M_2 and D_2.

Ordovician amphibole $^{40}Ar/^{39}Ar$ ages have also been obtained for metagabbro and mafic schist units of the Advocate Complex ophiolite and its tectonically imbricated early ophiolite cover indicating that they were subjected to Taconic tectonometamorphism. Amphibole analyses yielded ages varying between 481 and 465 Ma. The undisturbed plateaus produced the younger ages of the interval that are compatible with the data from the underlying Birchy Complex. The older and slightly disturbed spectrum giving an age of ca. 481 Ma suggests an early metamorphic event, shortly after crystallization of the gabbro at 483 Ma. A more ambiguous amphibole analysis of 453.5 ± 8.6 Ma was obtained from a gabbro located in a higher structural panel of the Advocate ophiolite. The plateau, characterized by a large step (68% gas released; apparent age of 452 ± 9 Ma) followed by less precise high temperature steps with apparent ages of up to 478 Ma, may hide mixed components of radiogenic argon, and is thus interpreted as providing a minimum age constraint of the amphibole aliquot. Together these Tremadocian to Darriwilian (Ordovician) ages are interpreted as recording the protracted nature of the Taconic M_1 metamorphism at the leading edge of the BVOT (Advocate Complex), the later part of which apparently cooled penecontemporane-

ously with that of the structurally underlying Birchy Complex.

The ca. 440 Ma amphibole age (08SNBT130) from the East Pond Metamorphic Suite represents an intermediate between the M_1 and M_2 age constraints of the Advocate and Birchy complexes. It is also older than the previously published ages for the Fleur de Lys Supergroup (ca. 428–374 Ma; Dallmeyer and Hibbard 1984; Cawood et al. 1995). There is no evidence in any of the heating steps for trapped excess ^{40}Ar, to which anomalously old ages can be attributed and recognized from examining inverse isochron plots (Kelley 2002). The age plateau is very well-defined and is concordant with the inverse isochron age ($^{40}Ar/^{36}Ar$ = 295.5, plot not shown). Therefore, the analyzed aliquot is likely not part of an M_2 amphibole paragenesis that incorporated extraneous Ar, nor, because of its fairly flat plateau, does it represent a partly recrystallized or slowly cooled M_1 amphibole. One interpretation is that the data reflect relatively fast cooling after a prolonged post M_1 burial period (465–440 Ma).

U–Pb Age and Trace Element Geochemistry

Type I and Type II zircon is considered to be metamorphic in origin, based on its habit, microstructural textures, mineral inclusions and geochemistry. Type I and II zircon includes some high Th/U values (e.g. >1; Table 3B) that are more common in igneous rocks (e.g. Rubatto 2002). However, Type I zircon has mineral inclusions of metamorphic mineral phases including epidote and clinozoisite, indicating that they must be metamorphic zircon grains. Trace element geochemical signatures of zircon are strongly influenced by garnet, because garnet preferentially incorporates the bulk of the rock's HREE budget into its crystal structure, leaving zircon and all other syn- and post-genetic phases relatively depleted in HREE (Rubatto 2002; Rubatto and Hermann 2003; Gilotti et al. 2004, Skublov et al. 2012). In contrast, metamorphic zircon growing in the presence of garnet is greatly enriched in Hf relative to garnet with published $^{Hf}D_{Zrn/Grt}$ values in the range 24,085–170,739 (Rubatto 2002). Type I zircon has HREE-enriched chondrite

profiles (Fig. 10) typical of zircon that did not form in the presence of garnet, which preferentially retains the HREE. Only one Type I zircon grain (188.T1 Fig. 10) has a negative Eu anomaly suggesting that minor amounts of residual plagioclase may have been present when this zircon was growing (Rubatto 2002). Type II zircon has all the characteristics of zircon that has grown in the presence of garnet (Rubatto 2002): it has flat, low HREE profiles, is depleted in Y, and is significantly enriched in Hf relative to Type 1 zircon (Table 3B; Fig. 10). Furthermore, none of the Type II zircon grains have negative Eu anomalies, suggesting plagioclase was largely absent during their growth.

The enrichment of HREE relative to the MREE in Type I zircon means that metamorphic growth of Type I zircon either predated the main phase of garnet growth and eclogitic-facies metamorphism, or that it took place during and/or after garnet had started to break down (almost completely) and released HREE back into the bulk rock. The latter is the preferred interpretation because Type I zircon is spatially associated with retrograde assemblage phases such as amphibole, epidote and quartz, and the inclusions identified in Type I zircon comprise epidote, clinozoisite, quartz, amphibole, and very rare relict clinopyroxene. We propose that Type I zircon grew at 465 ± 12 Ma on the M_1 retrograde path during garnet break down following eclogite-facies metamorphism. This is consistent with the interpretation of Stallard and Hickey (2002) that the first stage of garnet growth (their G1) in the Fleur de Lys Supergroup ceased and garnet consumption began following the Early Ordovician Taconic metamorphism. The flat HREE patterns of Type II zircon resemble the compositional profiles for zircon that formed either syn- or post-garnet growth. These low U zircon grains and narrow overgrowths could not be dated. We tentatively interpret that they crystallized during Salinic M_2 metamorphism when growth of new garnet phases resumed (analogous to the G2 to G4 garnet growth phases of Stallard and Hickey 2002) under amphibolite-facies conditions.

DISCUSSION OF THE TECTONIC IMPLICATIONS OF THE NEW AGE DATA

Previous geochronologic investigations obtained predominantly Silurian Salinic ages for tectonometamorphism along the Baie Verte Line in Newfoundland and called into question the intensity and nature of Taconic orogenesis (Cawood et al. 1994) despite the structural, petrological and sedimentological evidence for Ordovician Taconic tectonism (e.g. Dallmeyer 1977; Cawood and Suhr 1992; van Staal et al. 2007). Our data on the Birchy Complex, Advocate Complex and the East Pond Metamorphic Suite indicate that the evidence for Taconic orogeny is locally preserved, but is extensively overprinted elsewhere. The discovery of Taconic tectonometamorphism on the Baie Verte Peninsula provides critical information on the closure of the Taconic seaway, the terminal collision between the Notre Dame arc and the Humber margin, and subsequent tectonometamorphic events (Fig. 11).

Taconic Orogeny

The Advocate Complex and associated members of the BVOT record Late Cambrian (~489 Ma) subduction initiation and hence, the onset of the seaway closure (van Staal et al. 2007, 2013; Fig. 11A). The BVOT ophiolites occupied the upper plate during the collision and were obducted onto the Humber margin. As they remained in the upper plate throughout much of their history, they are the most likely to preserve the oldest ages associated with initial stages of the Taconic arc–continent collision. This proposition is supported by the age relationships between the BVOT and its unconformable cover of the Snooks Arm Group: the interpreted unconformity at the base of the Snooks Arm Group near the Baie Verte Line (Skulski et al. 2010), and presence of ophiolite-derived detritus in <479 Ma to >476 Ma, lower Snooks Arm Group conglomerate and sedimentary breccia (Kidd 1974; Skulski et al. 2010) suggests local emergence of the BVOT during initial stages of collision at that time. The $^{40}Ar/^{39}Ar$ plateau ages from a strained metagabbro and mafic schist of the Advocate Complex range from 481–465 Ma and suggest that parts of

Table 3. Major element, trace and rare earth element geochemistry for sample SNB-06-020

Table 3A. Whole rock major element geochemistry and selected trace elements[a] for sample SNB-06-020

Sample	SiO_2	TiO_2	Al_2O_3	FeO	MnO	MgO	CaO	Na_2O	K_2O	P_2O_5	TOTAL	Co	Cr_2O_3	Ni	V
	wt%											ppm			
SNB-06-020	48.8	1.34	14.31	12.7	0.22	7.69	12.0	2.17	0.23	0.14	99.5	45	403	107	322

a: Major elements and selected trace elements (Co, Cr_2O_3, Ni and V) for the whole rock sample were analyzed by X-ray fluorescence spectrometry at the McGill University Geochemical Laboratories. The samples were jaw crushed, hand-picked, ground in an alumina shatter box, and fused into 32 mm-diameter beads prepared from a 1:5 mixture of a sample and lithium tetraborate ($B_4Li_2O_7$). Analyses were conducted by a PHILIPS PW2440, 4kW automated XRF spectrometer using a-coefficient technique. Major-element instrumental precision is within 0.23% relative to stated values, and the overall analytical precision is within 0.5%. The accuracy for SiO_2 is within 0.5%, for other major elements within 1%, and for the selected trace elements within 5% of stated values.

Table 3B. Zircon and whole rock trace and rare earth element data[b] for sample SNB-06-020

Labels[c]	Ta	Y	Ba	La	Ce	Pr	Nd	Sm	Eu	Gd	Tb	Dy	Ho	Er	Tm	Yb	Lu	Hf	Th	U	Yb/Sm	Yb/Gd	Th/U	Lu/Sm	Apparent SHRIMP Age (Ma)	Comment[d]	Zircon Type[e]
9536-188.T1	4.71	4866	66.02	0.55	34.3	0.112	3.01	1.55	2.0	75.8	25.4	361.5	143.8	515	168.9	1597	340.5	6879	2569	2335	125	25	1.100	178	477 ± 10	along contact btw qtz, amph, rut	I
9536-961.T1	0.87	86	0.138	bdl	0.1	0.005	bdl	bdl	0.1	0.5	0.4	7.3	2.6	10	1.6	12.5	1.3	12459	0.03	1.5	--	31	0.017	--	--	along contact with cpx-rut	II
9536-311.T1	1.43	2107	4.606	0.07	12.0	0.069	1.0	4.74	2.2	32.7	11.8	209.0	80.8	366	80.14	761.1	137.0	4698	121.46	219.9	145	28	0.552	174	483 ± 9, 455 ± 9	entirely within amph	I
9536-944.T1	3.21	805	3.584	0.14	0.6	0.055	0.4	0.31	0.2	1.9	1.4	35.0	24.1	162	40.9	472.4	93.5	5961	16.13	85.5	1352	308	0.189	1791	447 ± 10	along contact btw ep-qtz	I
9536-944.T2	0.33	13	0.633	0.12	2.1	0.130	bdl	0.10	0.1	0.2	0.1	1.2	0.5	3	0.5	3.7	0.8	13154	0.24	0.1	32	22	1.600	47	--	along contact btw ep-qtz	II
9536-133.T1	2.29	274	2.693	1.35	13.9	1.032	3.5	3.16	1.2	5.0	0.9	17.8	9.3	52	15.25	151.9	30.5	6524	16.44	31.6	43	37	0.520	58	448 ± 22	btw grt grains, in ep-amph matrix	I/II
9536-380.T1	6.36	756	38.41	0.07	0.5	0.045	0.5	6.51	0.1	31.4	6.5	92.1	32.8	186	41.34	478.7	120.9	6221	72.91	173.1	66	18	0.421	112	449 ± 16	along contact btw grt-amph	I
9536-560.T1	0.4	167	149.3	0.01	0.3	0.052	0.1	0.13	0.1	1.5	0.7	11.0	5.9	37	11.29	114.2	16.2	6390	28.81	26.1	795	93	1.102	754	442 ± 24	along contact btw amph-ep-qtz	I/II
9536-603.T1	1.25	28	1.849	0.76	2.5	0.280	1.6	0.03	0.1	0.1	0.1	1.9	0.8	3	0.6	5.9	0.8	13235.8	0.08	0.4	183	55	0.198	164	--	entirely within amph	II
SNB-06-020[f]	0.29	27	51	4.81	11.4	1.81	9.53	3.04	1.2	3.92	0.69	4.45	0.95	2.93	0.4	2.8	0.4	1.7	0.36	0.1	0.8	0.9	3.273	0.8	--	--	---

b: Element abundances reported in ppm. Yb/Sm, Yb/Gd, and Lu/Sm values are chondrite-normalized after Sun and McDonough (1989)

c: Spot name follows the convention x-y.Tz; where x = sample number, y = zircon grain number, T denotes a trace element analysis, and z = spot number.

d: btw: between, ep: epidote, qtz: quartz, cpx: clinopyroxene, amph: amphibole, grt: garnet, rut: rutile

e: Where zircon Type is noted as I/II, the analytical spot fell partially in a Type I core and a Type II overgrowth

f: Whole rock trace elements were analyzed by ICP-MS at Actlabs (Ancaster, Ontario), using the 4B2 research protocol. Samples were prepared using a lithium metaborate/tetraborate fusion method and were analyzed using a Perkin Elmer SCIEX ELAN 9000 ICP/MS. Detection limits are (in ppm): Ta (0.01), Y (0.5), Ba (3), La (0.05), Ce (0.05), Pr (0.01), Nd (0.05), Sm (0.01), Eu (0.005), Gd (0.01), Tb (0.01), Dy (0.01), Ho (0.01), Er (0.01), Tm (0.005), Yb (0.01), Lu (0.002), Hf (0.1), Th (0.05), and U (0.01)
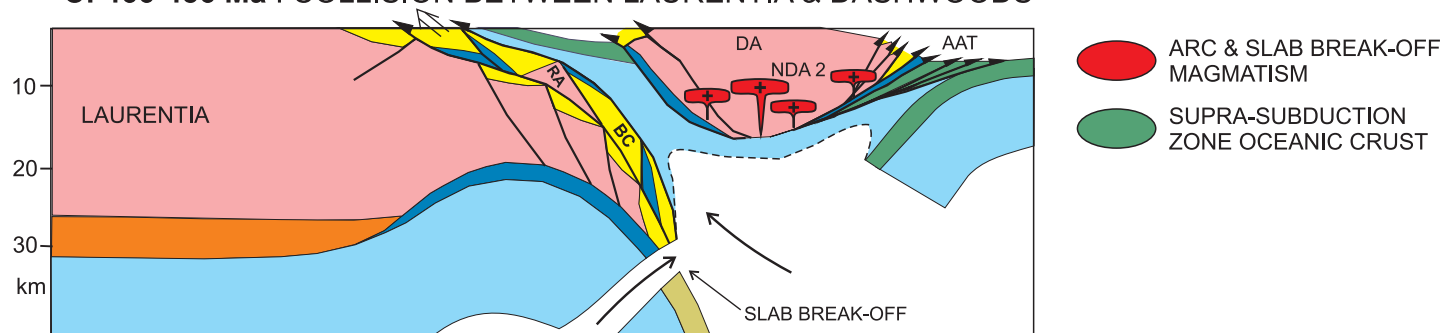
bdl: below detection limit
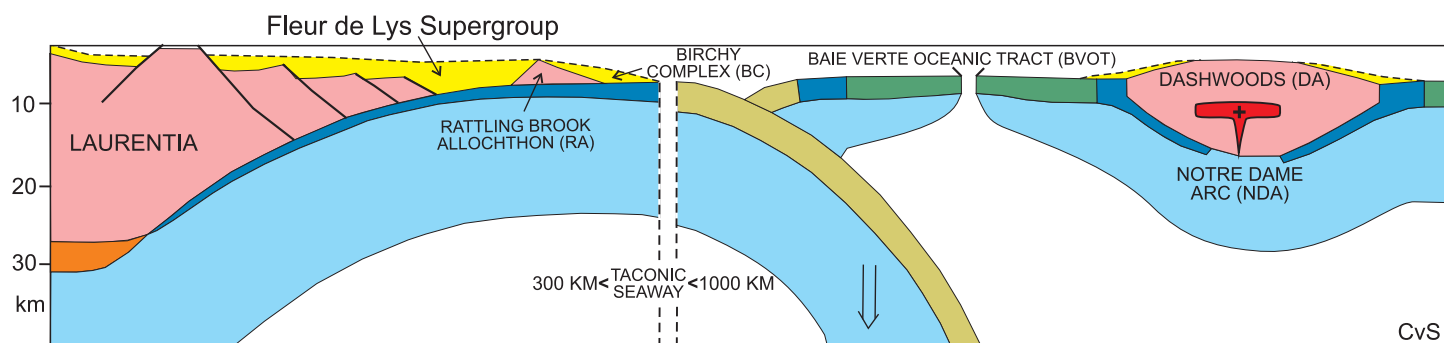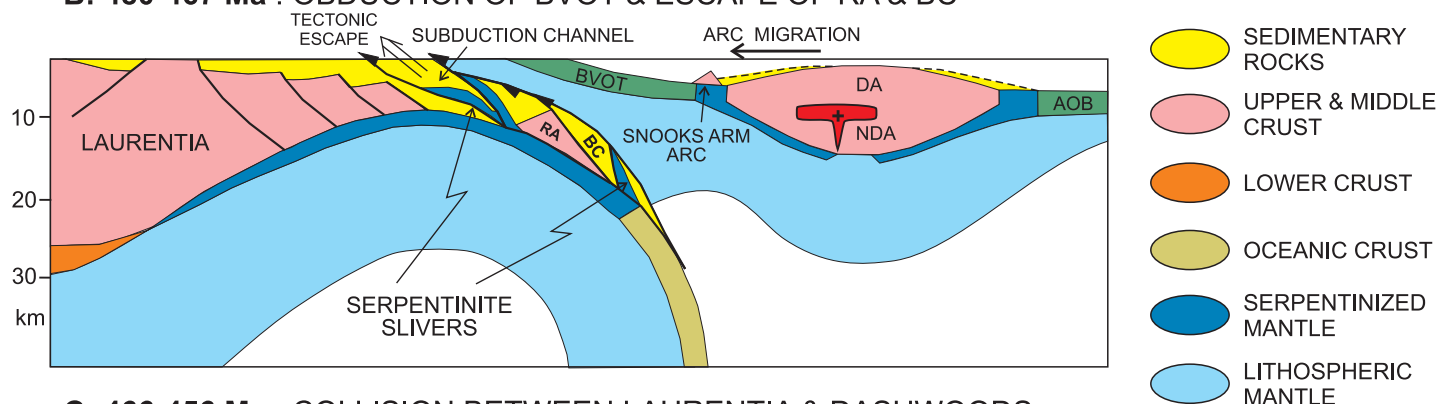
Figure 11. Schematic tectonic evolution of the closure of the Taconic sea-way and the Notre Dame arc–Laurentia collision between 490 and 456 Ma. These figures are a continuation of Figure 9 of van Staal et al. (2013), which illustrated the progressive hyperextension of the Humber margin with exhumation of lithospheric continental mantle onto the seafloor and the subsequent spreading that led to formation of the oceanic Taconic sea-way and isolation of Dashwoods. A: Initiation of east-directed subduction in the Taconic sea-way at ca. 490 Ma, which led to suprasubduction zone spreading and formation of the boninitic ophiolites of the Baie Verte oceanic tract (BVOT) and first phase of the Notre Dame arc (489–476 Ma). The BVOT became basement to the forearc basin attached to the Notre Dame arc, as indicated by ample continental arc fragments in the basal part of the Flat Water Pond/Snooks Arm groups deposited above the BVOT (Skulski et al. 2010). B: Start of the Taconic collision. Entrance and partial escape of former extensional allochthons (Rattling Brook allochthon) and transitional oceanic crust (Birchy Complex) of the hyperextended Humber margin of Laurentia into a progressively widening subduction channel. The hanging wall lid of the subduction channel is the partially obducted BVOT. Progressive steepening of the down-going Humber margin slab caused arc magmatism to locally migrate onto the BVOT, forming the 476–467 Ma extensional Snooks Arm arc. Onset of collision had initiated west-directed subduction east of Dashwoods (outside picture) forming the suprasubduction zone Annieopsquotch ophiolite belt (AOB, van Staal et al. 2007). C: Further steepening of the down-going slab, full-scale collision between Dashwoods and Humber margin, obduction of the BVOT onto the margin platform and further escape of the Rattling Brook allochthon and Birchy Complex above the closure temperature for argon diffusion in white mica. Magmatism following influx of asthenosphere after slab break-off took place in Dashwoods and locally in the obducted BVOT. West-directed subduction east of Dashwoods formed the Annieopsquotch accretionary tract (AAT).

this unit were also deformed during the Taconic collision. The ca. 483 Ma protolith of the metagabbro intruded during the formation of the early ophiolite cover sequence and may have been tectonically imbricated with the Advocate Complex during early obduction. Hence, the metagabbro and mafic schist do not represent remnants of a metamorphic sole, but rather a plutonic rock that was dismembered in the shear zone that separates the mantle tectonites from the crustal units of the Advocate complex (see Bursnall 1975 and Hibbard 1983). Kinematics of this shear zone are complex because it accommodated several phases of shear as indicated by overprinting relationships (Bursnall 1975). Based on lithotectonic relationships (mantle tectonites at the base of the Duck Island Cove sequence overlying the Marble Cove sequence), we interpret the shear zone and the mafic schist to have formed initially during D_1 thrusting. Hence, the 481 Ma hornblende age probably records the first increments of deformation and regional metamorphism within the BVOT, which we ascribe to the early stages of BVOT obduction onto the Humber margin (Fig. 11B). Such an interpretation is consistent with the age relationships between the BVOT and its <479 Ma to >476 Ma unconformable cover (Skulski et al. 2010). Early Ordovician obduction of the BVOT is also supported by the presence of metamorphic zircon overgrowths in Mesoproterozoic basement rocks of the Humber margin which yielded a U–Pb age of 482.9 ± 8.5 Ma (de Wit and Armstrong 2014). All available age constraints thus indicate that underthrusting of the leading edge of the extended Humber margin started by at least ca. 480 Ma.

The Birchy Complex and East Pond Metamorphic Suite form part of the late Ediacaran hyperextended Humber margin that formed during the opening of the Taconic Seaway (van Staal et al. 2013). Metamorphic studies suggest that the Birchy Complex and related units of the Humber margin, and especially its Mesoproterozoic basement (de Wit and Armstrong 2014), were subducted to relatively deep levels beneath the BVOT and adjacent Notre Dame arc during the

Taconic arc–continent collision (East Pond Metamorphic Suite estimates at minimum 7–12 kbar in Jamieson 1990, and up to 18–20 kbar in Willner et al. 2012). Our new ages provide evidence that deformation and metamorphism associated with this event (D_1) took place during the Early to Middle Ordovician Taconic, rather than during the Silurian Salinic orogeny as was inferred previously (e.g. Cawood et al. 1994; Waldron et al. 1998). The U–Pb zircon age of 465 ± 12 Ma for the amphibolitized eclogite of the East Pond Metamorphic Suite provides an additional minimum age for the start of the Taconic collision. The metamorphic zircon growth in the eclogite is interpreted to have occurred during the initial stages of exhumation, during the first stages of retrograde growth of hornblende. The similarity in metamorphic ages between the Birchy Complex and the East Pond Metamorphic Suite eclogite indicates that subduction of the Humber margin (A-subduction) was not restricted to the Birchy Complex at its leading edge, but probably involved a significant segment of this margin (Fig. 11).

Rapid exhumation of the Birchy complex is indicated by similar muscovite and hornblende ^{40}Ar/^{39}Ar ages (ca. 466 Ma) from the same sample. ^{40}Ar/^{39}Ar ages from the Birchy Complex (467–461 Ma) closely overlap with the age constraints on syn-collision magmatism (465–459 Ma) associated with break-off of the oceanic slab (Taconic seaway) attached to the Humber margin (van Staal et al. 2007; Fig. 11B and C). Thus, this exhumation occurred during the terminal stages of the Taconic collision between the Humber margin and the Notre Dame arc. These constraints are consistent with a model involving buoyancy-driven delamination, stacking and extrusion of the Birchy Complex in the A-subduction channel as driving mechanisms for rapid exhumation during terminal collision (van Staal et al. 2013). Syn- to post-collision exhumation in the East Pond Metamorphic Suite was significantly more protracted and resulted in growth of retrograde amphibolite-facies mineral assemblages, which occurred prior to the 440 Ma hornblende cooling age.

Correlative Metamorphic Tectonites in the Northern Appalachians and Caledonides
Correlative units of the Appalachian–Caledonide orogen have locally preserved similar isotopic ages providing evidence for Taconic metamorphism and suggesting that analogous tectonic and exhumation processes have been active elsewhere along the Humber margin. ^{40}Ar/^{39}Ar ages from the locally eclogitic Tillotson Peak Complex and amphibolitic Belvidere Mountain Complex in northern Vermont, of which the latter has some lithological affinities with the Birchy Complex, have preserved some of the earliest tectonometamorphic imprint documented in the northern Appalachians (505 to 460 Ma; Laird et al. 1984; Castonguay et al. 2012). ^{40}Ar/^{39}Ar data from the Quebec Appalachians (496–461 Ma; Whitehead et al. 1995, 1996; Castonguay et al. 2001, 2007; Tremblay et al. 2011; De Souza et al. 2012) obtained from BVOT ophiolite (e.g. Thetford Mines, Lac Brompton), the Pennington Sheet (a possible correlative to the Birchy Complex) and from schist and amphibolite units of the Humber margin metamorphic units, all indicate a complex Furongian to Middle Ordovician orogenic event preceding a strong Silurian metamorphic overprint. Data from ophiolitic and Humber margin units of the Grampian orogen in the Scottish and Irish Caledonides (499–465 Ma; e.g. Chew et al. 2010) also clearly advocate for Taconic-related ophiolite obduction, collisional thickening and exhumation.

Salinic Tectonometamorphic Overprint
In the Baie Verte Peninsula, the Salinic orogeny is interpreted to have been associated with renewed crustal thickening of the Humber margin and BVOT causing D_{2-3} deformation and peak (temperature) regional metamorphism (Jamieson 1990; Cawood et al. 1995; Waldron et al. 1998; Skulski et al. 2010). The nature of the D_{2-3} deformation is apparently bivergent across the Baie Verte Line: northwest-verging in the Fleur de Lys Supergroup and southeast- to southwest-directed in the BVOT and cover rocks to the east (Kidd 1974; Bursnall 1975; Hibbard

1983; Fig. 2). The Birchy and Advocate complexes apparently occupy the axial region of this structurally complex thrust belt, which may explain, in part, why they have escaped significant metamorphic overprint during the Silurian. The time span of D_{2-3} and formation of large, upright basement-cored F_2 folds is constrained by intrusion of the ca. 428 Ma Wild Cove Pond Igneous Suite, which is locally affected by S_2 but also cuts across D_2 structures, and by the post-D_3 ca. 423 Ma Trap Pond pluton (Kidd 1974; Hibbard 1983; Skulski et al. 2012b). Such evidence and the associated ca. 428 Ma migmatite (Cawood and Dunning 1993; Skulski et al. 2012b) suggest that composite D_{2-3} is Salinic and it took place during the Wenlock–Ludlow. The ca. 425 Ma muscovite age (this study) from a psammite with penetrative S_2 in the Birchy Complex probably represents a D_2 cooling age and indicates that large parts of the Fleur de Lys Supergroup had cooled down below the closure temperature of white mica by the end of the Silurian.

CONCLUSION
The Birchy and Advocate complexes of the Newfoundland Appalachians partly preserve a complex tectonic evolution characterized by the late Ediacaran opening of the Taconic Seaway and its Early to Mid Ordovician closure leading to partial subduction and exhumation of an ocean–continent transition zone and ophiolite obduction of the Baie Verte oceanic tract onto the Humber margin during Taconic orogenesis.

New $^{40}Ar/^{39}Ar$ ages (481–461 Ma) of amphibole and micas from the Advocate Complex (obducted ophiolite of the BVOT) and underlying Birchy Complex (ocean–continent transition zone), combined with an amphibole $^{40}Ar/^{39}Ar$ age (440 ± 3.4 Ma) and *in situ* U–Pb zircon age (465 ± 12 Ma) of an amphibolitized eclogite from the remobilized basement of the Fleur de Lys Supergroup (East Pond Metamorphic Suite), confirm significant Taconic burial and tectonometamorphism of these units prior to significant Silurian (Salinic) overprint. Moreover, the preservation of these metamorphic ages and early metamorphic paragenesis in spite of an otherwise penetrative Salinic

overprint advocates for a mechanism, such as tectonic extrusion in a subduction channel, which would have accommodated rapid exhumation of the Birchy Complex to high structural levels, penecontemporaneously with obduction of the Advocate Complex during the Taconic orogenic cycle.

REFERENCES
Anderson, S.D., 1998, Structure, metamorphism, and U–Pb and $^{40}Ar/^{39}Ar$ geochronology of the Ming's Bight Group, and the Paleozoic tectonic evolution of the Baie Verte Peninsula, Newfoundland: Unpublished PhD thesis, Dalhousie University, Halifax, NS, 452 p.

Anderson, S.D., Jamieson, R.A., Reynolds, P.H., and Dunning, G.R., 2001, Devonian extension in Northwestern Newfoundland: $^{40}Ar/^{39}Ar$ and U–Pb data from the Ming's Bight Area, Baie Verte Peninsula: The Journal of Geology, v. 109, p. 191–211, http://dx.doi.org/10.1086/319237.

Bédard, J.H., Lauzière, K., Tremblay, A., Sangster, A., Douma, S.L., and Dec, T., 2000, Betts Cove ophiolite and its cover rocks, Newfoundland: Geological Survey of Canada, Bulletin 550, 76 p., http://dx.doi.org/10.4095/211642.

Black, L.P., Kamo, S.L., Allen, C.M., Davis, D.W., Aleinikoff, J.N., Valley, J.W., Mundil, R., Campbell, I.H., Korsch, R.J., Williams, I.S., and Foudoulis, C., 2004, Improved $^{206}Pb/^{238}U$ microprobe geochronology by monitoring of a trace-element-related matrix effect; SHRIMP, ID–TIMS, ELA–ICP–MS and oxygen isotope documentation for a series of zircon standards: Chemical Geology, v. 205, p. 115–140, http://dx.doi.org/10.1016/j.chemgeo.2004.01.003.

Bursnall, J.T., 1975, Stratigraphy, structure and metamorphism west of Baie Verte, Burlington Peninsula, Newfoundland: Unpublished PhD thesis, Cambridge University, England, 337 p.

Bursnall, J.T., and de Wit, M.J., 1975, Timing and development of the orthotectonic zone in the Appalachian orogen of northwest Newfoundland: Canadian Journal of Earth Sciences, v. 12, p. 1712–1722, http://dx.doi.org/10.1139/e75-152.

Castonguay, S., Ruffet, G., Tremblay, A., and Féraud, G., 2001, Tectonometamorphic evolution of the southern Quebec Appalachians: $^{40}Ar/^{39}Ar$ evidence for Middle Ordovician crustal thickening and Silurian–Early Devonian exhumation of the internal Humber Zone: Geological Society of America Bulletin, v. 113, p. 144–160, http://dx.doi.org/10.1130/0016-7606(2001)113<0144:TEOTSQ>2.0.CO;2.

Castonguay, S., Ruffet, G., and Tremblay, A., 2007, Dating polyphase deformation across low-grade metamorphic belts: An example based on $^{40}Ar/^{39}Ar$ muscovite age constraints from the southern Quebec Appalachians, Canada: Geological Society of America Bulletin, v. 119, p. 978–992, http://dx.doi.org/10.1130/B26046.1.

Castonguay, S., Skulski, T., van Staal, C.R., McNicoll, V., and Joyce, N., 2010, Structure and timing of deformation and metamorphism of the Baie Verte Peninsula, Newfoundland Appalachians (abstract), *in* Kerr, A., and Pereira, C., *eds.*, Annual Meeting Geological Association of Canada, Newfoundland and Labrador section, Program and Abstracts, p. 2.

Castonguay, S., Kim, J., Thompson, P.J., Gale, M.H., Joyce, N., Laird, J., and Doolan, B.L., 2012, Timing of tectonometamorphism across the Green Mountain anticlinorium, northern Vermont Appalachians: $^{40}Ar/^{39}Ar$ data and correlations with southern Quebec: Geological Society of America Bulletin, v. 124, p. 352–367, http://dx.doi.org/10.1130/B30487.1.

Cawood, P.A., and Dunning, G.R., 1993, Silurian age for movement on the Baie Verte Line: Implications for accretionary tectonics in the Northern Appalachians (abstract): Geological Society of America, Abstracts with Programs, v. 25, no. 6, p. A422.

Cawood, P.A., and Suhr, G., 1992, Generation and obduction of ophiolites: Constraints from the Bay of Islands Complex, western Newfoundland: Tectonics, v. 11, p. 884–897, http://dx.doi.org/10.1029/92TC00471.

Cawood, P.A., Dunning, G.R., Lux, D., and van Gool, J.A.M., 1994, Timing of peak metamorphism and deformation along the Appalachian margin of Laurentia in Newfoundland: Silurian, not Ordovician: Geology, v. 22, p. 399–402, http://dx.doi.org/10.1130/0091-7613(1994)022<0399:TOPMAD>2.3.CO;2.

Cawood, P.A., van Gool, J.A.M., and Dunning, G.R., 1995, Collisional tectonics along the Laurentian margin of the Newfoundland Appalachians: Geological Association of Canada, Special Paper, v. 41, p. 283–301.

Chew, D.M., Daly, J.S., Magna, T., Page, L.M., Kirkland, C.L., Whitehouse, M.J., and Lam, R., 2010, Timing of ophiolite obduction in the Grampian orogen: Geological Society of America Bulletin, v. 122, p. 1787–1799, http://dx.doi.org/10.1130/B30139.1.

Church, W.R., 1969, Metamorphic rocks of the Burlington Peninsula and adjoining areas of Newfoundland and their bearing on continental drift in the North Atlantic, in Kay, M., ed., North Atlantic Geology and Continental drift: American Association of Petroleum Geologists, Memoir 12, p. 212–233.

Dahl, P.S., 1996, The effects of composition on retentivity of argon and oxygen in hornblende and related amphiboles: A field-tested empirical model: Geochimica et Cosmochimica Acta, v. 60, p. 3687–3700, http://dx.doi.org/10.1016/0016-7037(96)00170-6.

Dallmeyer, R.D., 1977, $^{40}Ar/^{39}Ar$ age spectra of minerals from the Fleur de Lys terrane in northwest Newfoundland: Their bearing on chronology of metamorphism within the Appalachian orthotectonic zone: The Journal of Geology, v. 85, p. 89–103, http://dx.doi.org/10.1086/628270.

Dallmeyer, R.D., and Hibbard, J., 1984, Geochronology of the Baie Verte Peninsula, Newfoundland: Implications for the tectonic evolution of the Humber and Dunnage Zones of the Appalachian Orogen: The Journal of Geology, v. 92, p. 489–512, http://dx.doi.org/10.1086/628888.

De Souza, S., Tremblay, A., Ruffet, G., and Pinet, N., 2012, Ophiolite obduction in the Quebec Appalachians, Canada – $^{40}Ar/^{39}Ar$ age constraints and evidence for syn-tectonic erosion and sedimentation: Canadian Journal of Earth Sciences, v. 49, p. 91–110, http://dx.doi.org/10.1139/e11-037.

de Wit, M.J., 1980, Structural and metamorphic relationships of pre-Fleur de Lys and Fleur de Lys rocks of the Baie Verte Peninsula, Newfoundland: Canadian Journal of Earth Sciences, v. 17, p. 1559–1575, http://dx.doi.org/10.1139/e80-163.

de Wit, M.J., and Armstrong, R., 2014, Ode to Field Geology of Williams: Fleur de Lys nectar still fermenting on Belle Isle: Geoscience Canada, v. 41, p. 118–137, http://dx.doi.org/10.12789/geocanj.2014.41.043.

de Wit, M.J., and Strong, D.F., 1975, Eclogite-bearing amphibolites from the Appalachian Mobile Belt, northwest Newfoundland: Dry versus wet metamorphism: The Journal of Geology, v. 83, p. 609–627, http://dx.doi.org/10.1086/628144.

Dunning, G.R., and Krogh, T.E., 1985, Geochronology of ophiolites of the Newfoundland Appalachians: Canadian Journal of Earth Sciences, v. 22, p. 1659–1670, http://dx.doi.org/10.1139/e85-174.

Gilotti, J.A., Nutman, A.P., and Brueckner, H.K., 2004, Devonian to Carboniferous collision in the Greenland Caledonides: U–Pb zircon and Sm–Nd ages of high-pressure and ultrahigh-pressure metamorphism: Contributions to Mineralogy and Petrology, v. 148, p. 216–235, http://dx.doi.org/10.1007/s00410-004-0600-4.

Goodwin, L.B., and Williams, P.F., 1996, Deformation path partitioning within a transpressive shear zone, Marble Cove, Newfoundland: Journal of Structural Geology, v. 18, p. 975–990, http://dx.doi.org/10.1016/0191-8141(96)00015-6.

Hacker, B.R., and Gerya, T.V., 2013, Paradigms, new and old, for ultrahigh-pressure tectonism: Tectonophysics, v. 603, p. 79–88, http://dx.doi.org/10.1016/j.tecto.2013.05.026.

Harrison, T.M., Célérier, J., Aikman, A.B., Hermann, J., and Heizler, M.T., 2009, Diffusion of ^{40}Ar in muscovite: Geochimica et Cosmochimica Acta, v. 73, p. 1039–1051, http://dx.doi.org/10.1016/j.gca.2008.09.038.

Hibbard, J., 1983, Geology of the Baie Verte Peninsula, Newfoundland: Mineral Development division Department of Mines and Energy, Government of Newfoundland and Labrador, Memoir 2, 279 p.

Hibbard, J.P., St. Julien, P., and Trzcienski, W.E., Jr., 1995, Humber Zone internal, in Williams, H., ed., Chapter 3 of Geology of the Appalachian–Caledonian Orogen in Canada and Greenland: Geological Survey of Canada, Geology of Canada, no. 6, p. 114–139.

Hibbard, J.P., van Staal, C.R., and Rankin, D.W., 2007, A comparative analysis of pre-Silurian crustal building blocks of the northern and southern Appalachian orogen: American Journal of Science, v. 307, p. 23–45, http://dx.doi.org/10.2475/01.2007.02.

Jamieson, R.A., 1990, Metamorphism of an Early Palaeozoic continental margin, western Baie Verte Peninsula, Newfoundland: Journal of Metamorphic Geology, v. 8, p. 269–288, http://dx.doi.org/10.1111/j.1525-1314.1990.tb00473.x.

Jamieson, R.A., and Beaumont, C., 2013, On the origin of orogens: Geological Society of America Bulletin, v. 125, p. 1671–1702, http://dx.doi.org/10.1130/B30855.1.

Jamieson, R.A., and O'Beirne-Ryan, A.M., 1991, Decompression-induced growth of albite porphyroblasts, Fleur de Lys Supergroup, western Newfoundland: Journal of Metamorphic Geology, v. 9, p. 433–439, http://dx.doi.org/10.1111/j.1525-1314.1991.tb00537.x.

Jamieson, R.A., and Vernon, R.H., 1987, Timing of porphyroblast growth in the Fleur de Lys Supergroup, Newfoundland: Journal of Metamorphic Geology, v. 5, p. 273–288, http://dx.doi.org/10.1111/j.1525-1314.1987.tb00384.x.

Kelley, S., 2002, Excess argon in K–Ar and Ar–Ar geochronology: Chemical Geology, v. 188, p. 1–22, http://dx.doi.org/10.1016/S0009-2541(02)00064-5.

Kennedy, M.J., 1971, Structure and stratigraphy of the Fleur de Lys Supergroup in the Fleur de Lys area, Burlington Peninsula, Newfoundland: Geological Association of Canada, Proceedings 24, p. 59–71.

Kidd, W.S.F., 1974, The evolution of the Baie Verte lineament, Burlington Peninsula, Newfoundland: Unpublished PhD thesis, University of Cambridge, Cambridge, England, 294 p.

Kuiper, K.F., Deino, A., Hilgen, F.J., Krijgsman, W., Renne, P.R., and Wilbrans, J.R., 2008, Synchronizing rock clocks

of earth history: Science, v. 320, p. 500–504, http://dx.doi.org/ 10.1126/science.1154339.

Laird, J., Lanphere, M.A., and Albee, A.L., 1984, Distribution of Ordovician and Devonian metamorphism in mafic and pelitic schists from northern Vermont: American Journal of Science, v. 284, p. 376–413, http://dx.doi.org/ 10.2475/ajs.284.4-5.376.

Lin, S., Brem, A.G., van Staal, C.R., Davis, D.W., McNicoll, V.J., and Pehrsson, S., 2013, The Corner Brook Lake block in the Newfoundland Appalachians: A suspect terrane along the Laurentian margin and evidence for large-scale orogen-parallel motion: Geological Society of America Bulletin, v. 125, p. 1618–1632, http://dx.doi.org/10.1130/B30805.1.

Ludwig, K.R., 2003, User's manual for Iso- plot/Ex 3.00: A geochronological toolkit for Microsoft Excel: Berkeley Geochronology Center, Special Publi- cation 4, 70 p.

Mattinson, J.M., 1977, U–Pb ages of some crystalline rocks from the Burlington Peninsula, Newfoundland, and impli- cations for the age of Fleur de Lys metamorphism: Canadian Journal of Earth Sciences, v. 14, p. 2316–2324, http://dx.doi.org/10.1139/e77-199.

Min K., Mundil, R., Renne, P.R., and Lud- wig, K.R., 2000, A test for systematic errors in ^{40}Ar/^{39}Ar geochronology through comparison with U/Pb analy- sis of a 1.1-Ga rhyolite: Geochimica Cosmochimica Acta, v. 64, p. 73–98, http://dx.doi.org/10.1016/S0016- 7037(99)00204-5.

Neale, E.R.W., and Kennedy, M.J., 1967, Relationship of the Fleur de Lys Group to other groups of the Burlington Peninsula, Newfoundland, *in* Neale, E.R.W., and Williams, H., *eds.*, Geology of the Atlantic Region: Geological Association of Canada, Special Paper 4, p. 139–169.

Neale, E.R.W., Kean, B.F., and Upadhyay, H.D., 1975, Post-ophiolite unconfor- mity, Tilt Cove–Betts Cove area, New- foundland: Canadian Journal of Earth Sciences, v. 12, p. 880–886, http://dx.doi.org/10.1139/e75-077.

Piasecki, M.A.J., 1988, Strain-induced min- eral growth in ductile shear zones and a preliminary study of ductile shearing in western Newfoundland: Canadian Journal of Earth Sciences, v. 25, p. 2118–2129, http://dx.doi.org/10.1139/e88-195.

Ramezani, J., 1993, The geology, geochem- istry and U–Pb geochronology of the Stog'er Tight gold prospect, Baie Verte Peninsula, Newfoundland:

Unpublished MSc thesis, Memorial University of Newfoundland, St. John's, NL, 312 p.

Rayner, N.M., and Stern, R.A., 2002, Improved sample preparation for SHRIMP analysis of delicate mineral grains exposed in thin sections, *in* Radiogenic Age and Isotopic Studies, Report 15: Geological Survey of Canada, Current Research, F10, 3 p.

Roddick, J.C., 1988, The assessment of errors in ^{40}Ar/^{39}Ar dating, *in* Radi- ogenic Age and Isotopic Studies, Report 2: Geological Survey of Cana- da, Paper 88–2, p. 7–16.

Rubatto, D., 2002, Zircon trace element geochemistry: partitioning with garnet and the link between U–Pb ages and metamorphism: Chemical Geology, v. 184, p. 123–138, http://dx.doi.org/ 10.1016/S0009-2541(01)00355-2.

Rubatto, D., and Hermann, J., 2003, Zircon formation during fluid circulation in eclogites (Monviso, Western Alps): implications for Zr and Hf budget in subduction zones: Geochimica et Cos- mochimica Acta, v. 67, p. 2173–2187, http://dx.doi.org/10.1016/S0016- 7037(02)01321-2.

Scaillet, S., 2000, Numerical error analysis in ^{40}Ar/^{39}Ar dating: Chemical Geology, v. 162, p. 269–298, http://dx.doi.org/ 10.1016/S0009-2541(99)00149-7.

Skublov, S.G., Berezin, A.V., and Berezh- naya, N.G., 2012, General relations in the trace-element composition of zir- cons from eclogites with implications for the age of eclogites in the Belo- morian Mobile Belt: Petrology, v. 20, p. 427–449, http://dx.doi.org/ 10.1134/S0869591112050062.

Skulski, T., Castonguay, S., McNicoll, V., van Staal, C.R., Kidd, W., Rogers, N., Morris, W., Ugalde, H., Slavinski, H., Spicer, W., Moussalam, Y., and Kerr, I., 2010, Tectonostratigraphy of the Baie Verte oceanic tract and its ophio- lite cover sequence on the Baie Verte Peninsula: Current Research, New- foundland and Labrador Department of Natural Resources, Geological Sur- vey Report 10-1, p. 315–335.

Skulski, T., Castonguay, S., McNicoll, V., van Staal, C., and Kidd, W.S.F., 2012a, Western Baie Verte Peninsula revisit- ed: From ophiolite obduction onto Laurentia, the Notre Dame continen- tal arc, to post-arc continental volcan- ism and the Salinic Orogeny (abstract): Geological Association of Canada – Mineralogical Association of Canada Joint Annual Meeting, Abstracts, v. 35.

Skulski, T., McNicoll, V., Whalen, J.B., Moussallam, Y., Dunning, G., Cas- tonguay, S., Cawood, P., Kidd, W.S.F.,

and van Staal, C., 2012b, Subduction to slab break-off transition recorded in the timing, composition and setting of Early Silurian volcanoplutonic complexes, Baie Verte Peninsula, Newfoundland (abstract): Geological Association of Canada – Mineralogical Association of Canada Joint Annual Meeting, Abstracts, v. 35.

Stacey, J.S., and Kramers, J.D., 1975, Approximation of terrestrial lead iso- tope evolution by a two-stage model: Earth and Planetary Science Letters, v. 26, p. 207–221, http://dx.doi.org/ 10.1016/0012-821X(75)90088-6.

Stallard, A., 1998, Episodic porphyroblast growth in the Fleur de Lys Super- group, Newfoundland: Timing relative to the sequential development of mul- tiple crenulation cleavages: Journal of Metamorphic Geology, v. 16, p. 711–728, http://dx.doi.org/ 10.1111/j.1525-1314.1998.00167.x.

Stallard, A., and Hickey, K., 2002, A com- parison of microstructural and chemi- cal patterns in garnet from the Fleur de Lys Supergroup, Newfoundland: Journal of Structural Geology, v. 24, p. 1109–1123, http://dx.doi.org/ 10.1016/S0191-8141(01)00095-5.

Stern, R.A., 1997, The GSC Sensitive High Resolution Ion Microprobe (SHRIMP): analytical techniques of zircon U–Th–Pb age determinations and performance evaluation, *in* Radi- ogenic Age and Isotopic Studies, Report 10: Geological Survey of Canada, Current Research, 1997-F, p. 1–31.

Stern, R.A., 2001, A new isotopic and trace-element standard for the ion microprobe: preliminary thermal ion- ization mass spectrometry (TIMS) U–Pb and electron-microprobe data, *in* Radiogenic Age and Isotopic Stud- ies, Report 14: Geological Survey of Canada, Current Research, F1, 11 p.

Stern, R.A., and Amelin, Y., 2003, Assess- ment of errors in SIMS zircon U–Pb geochronology using a natural zircon standard and NIST SRM 610 glass: Chemical Geology, v. 197, p. 111–142, http://dx.doi.org/10.1016/S0009- 2541(02)00320-0.

Sun, S.-S., and McDonough, W.F., 1989, Chemical and isotopic systematics of oceanic basalts: Implications for man- tle composition and processes, *in* Saunders, A.D., and Norry, M.J., *eds.*, Magmatism in the Ocean Basins: Geo- logical Society, London, Special Publi- cations, v. 42, p. 313–345, http://dx.doi.org/10.1144/GSL.SP.19 89.042.01.19.

Tremblay, A., Ruffet, G., and Bédard, J.H.,

2011, Obduction of Tethyan-type ophiolites – A case-study from the Thetford Mines ophiolitic Complex, Quebec Appalachians, Canada: Lithos, v. 125, p. 10–26, http://dx.doi.org/10.1016/j.lithos.2011.01.003.

Vance, D., and O'Nions, R.K., 1990, Isotopic chronometry of zoned garnets: growth kinetics and metamorphic histories: Earth and Planetary Science Letters, v. 97, p. 227–240, http://dx.doi.org/10.1016/0012-821X(90)90044-X.

van Staal, C.R., Whalen, J.B., McNicoll, V.J., Pehrsson, S., Lissenberg, C.J., Zagorevski, A., van Breemen, O., and Jenner, G.A., 2007, The Notre Dame arc and the Taconic Orogeny in Newfoundland: Geological Society of America Memoirs, v. 200, p. 511–552, http://dx.doi.org/10.1130/2007.1200(26).

van Staal, C.R., Chew, D.M., Zagorevski, A., McNicoll, V., Hibbard, J., Skulski, T., Castonguay, S., Escayola, M.P., and Sylvester, P.J., 2013, Evidence of Late Ediacaran hyperextension of the Laurentian Iapetan margin in the Birchy Complex, Baie Verte Peninsula, northwest Newfoundland: Implications for the opening of Iapetus, formation of peri-Laurentian microcontinents and Taconic–Grampian orogenesis: Geoscience Canada, v. 40, p. 94–117, http://dx.doi.org/10.12789/geocanj.2013.40.006.

Villa, I.M., 1998, Isotopic closure: Terra Nova, v. 10, p. 42–47, http://dx.doi.org/10.1046/j.1365-3121.1998.00156.x.

Villa, I.M., 2004, Geochronology of metamorphic rocks: Periodico di Mineralogia, v. 73, p. 259–271.

Villeneuve, M.E., and MacIntyre, D.G, 1997, Laser ^{40}Ar/^{39}Ar ages of the Babine porphyries and Newman Volcanics, Fulton Lake map area, west-central British Columbia, *in* Radiogenic Age and Isotopic Studies, Report 10, Geological Survey of Canada, Current Research, 1997-F, p. 131–139.

Villeneuve, M.E., Sandeman, H.A., and Davis, W.J., 2000, A method for the intercalibration of U–Th–Pb and ^{40}Ar/^{39}Ar ages in the Phanerozoic: Geochimica et Cosmochimica Acta: v. 64, p. 4017–4030, http://dx.doi.org/10.1016/S0016-7037(00)00484-1.

Waldron, J.W.F., and van Staal, C.R., 2001, Taconian orogeny and the accretion of the Dashwoods block: A peri-Laurentian microcontinent in the Iapetus Ocean: Geology, v. 29, p. 811–814, http://dx.doi.org/10.1130/0091-7613(2001)029<0811:TOATAO>2.0.CO;2.

Waldron, J.F.W., Anderson, S.D., Cawood, P.A., Goodwin, L.B., Hall, J., Jamieson, R.A., Palmer, S.E., Stockmal, G.S., and Williams, P.F., 1998, Evolution of the Appalachian Laurentian margin: Lithoprobe results in western Newfoundland: Canadian Journal of Earth Sciences, v. 35, p. 1271–1287, http://dx.doi.org/10.1139/e98-053.

Whitehead, J., Reynolds, P.H., and Spray, J.G., 1995, The sub-ophiolitic metamorphic rocks of the Quebec Appalachians: Journal of Geodynamics, v. 19, p. 325–350, http://dx.doi.org/10.1016/0264-3707(94)00021-M.

Whitehead, J., Reynolds, P.H., and Spray, J.G., 1996, ^{40}Ar/^{39}Ar age constraints on Taconian and Acadian events in the Quebec Appalachians: Geology, v. 24; p. 359–362, http://dx.doi.org/10.1130/0091-7613(1996)024<0359:AAACOT>2.3.CO;2.

Williams, H., 1977, Ophiolitic mélange and its significance in the Fleur de Lys Supergroup, northern Appalachians: Canadian Journal of Earth Sciences, v. 14, p. 987–1003, http://dx.doi.org/10.1139/e77-091.

Williams, H., and St. Julien, P., 1982, The Baie Verte–Brompton Line; early Paleozoic continent–ocean interface in the Canadian Appalachians: Geological Association of Canada, Special Paper 24, p. 177–207.

Williams, H., Colman-Sadd, S.P., and Swinden, H.S., 1988, Tectonic-stratigraphic subdivisions of central Newfoundland: Geological Survey of Canada, Paper 88-1B, p. 91–98.

Willner, A.P., Massonne, H., van Staal, C.R., and Zagorevski, A., 2012, Contrasting PT-evolution during an Ordovician arc-continent collision at the Laurentian margin in western Newfoundland (abstract): Geological Association of Canada – Mineralogical Association of Canada, Joint Annual Meeting, St. John's 2012, Program with Abstracts, p. 152.

Winchester, J.A., Williams, H., Max, M.D. and van Staal, C.R, 1992, Does the Birchy Complex of Newfoundland extend into Ireland?: Journal of the Geological Society, v. 149, p. 159–162, http://dx.doi.org/10.1144/gsjgs.149.2.0159.